

# *AOI[3]: Smart Refractory Sensor Systems for Wireless Monitoring of Temperature, Health, and Degradation of Slagging Gasifiers*

## **Team:**

Dr. Debangsu Bhattacharyya <sup>b</sup>

Dr. David Graham <sup>c</sup>

Dr. Vinod Kulathumani <sup>c</sup>

Mr. Marc Palmisiano <sup>d</sup>

Dr. Edward M. Sabolsky <sup>a</sup>

<sup>a</sup>Department of Mechanical and Aerospace Engineering, WVU

<sup>b</sup>Department of Chemical Engineering, WVU

<sup>c</sup>Lane Department of Computer Science and Electrical Engineering, WVU

<sup>d</sup>HarbisonWalker International Technology Center



# Background- Gasifier Sensing Needs

- Online monitoring sensors of refractory used in coal gasifiers under extreme conditions including high temperature ( $>1300^{\circ}\text{C}$ ) and high pressure (up to 1000 psi) for  $>20,000$  hr.
- Erosive and corrosive conditions (due to slag and high pressure, in addition to various  $\text{pO}_2$  levels) causes degradation of refractory over time.
- Ability to monitor the integrity of the refractory materials during gasifier operation would contribute significantly to improving the overall operational performance and reliability of coal gasifiers.
  - Temperature
  - Stress/strain within refractory liner
  - Spallation events
  - Refractory liner health
- Monitoring interior thermochemical conditions allows for efficient control of the gasification process.

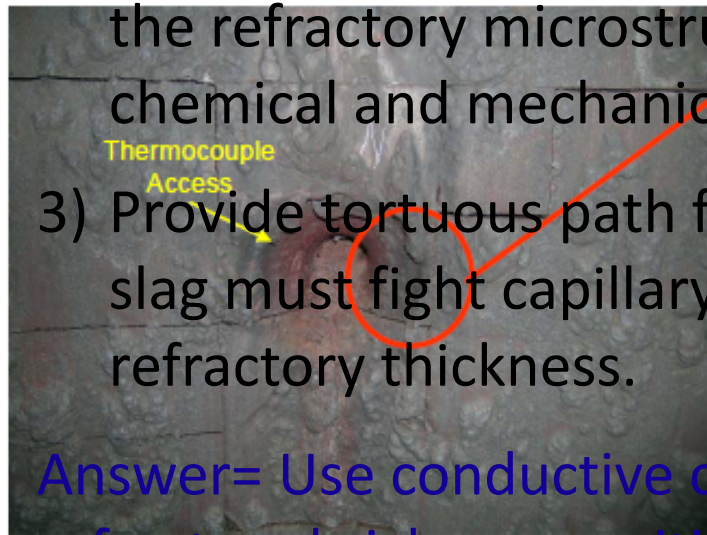


# Background- Gasifier Sensor Issues

## Edge Spalling/Corrosion of Refractory

### Where the Thermocouple Enters the Gasifier

- 1) Eliminate access port from the sensing design.
- 2) Incorporate sensing materials or structure within the refractory microstructure (retain refractory chemical and mechanical integrity).
- 3) Provide tortuous path for slag penetration, where slag must fight capillary forces to move through refractory thickness.



Answer= Use conductive ceramic composites with refractory brick composition as main constituent.



# Technology Vision

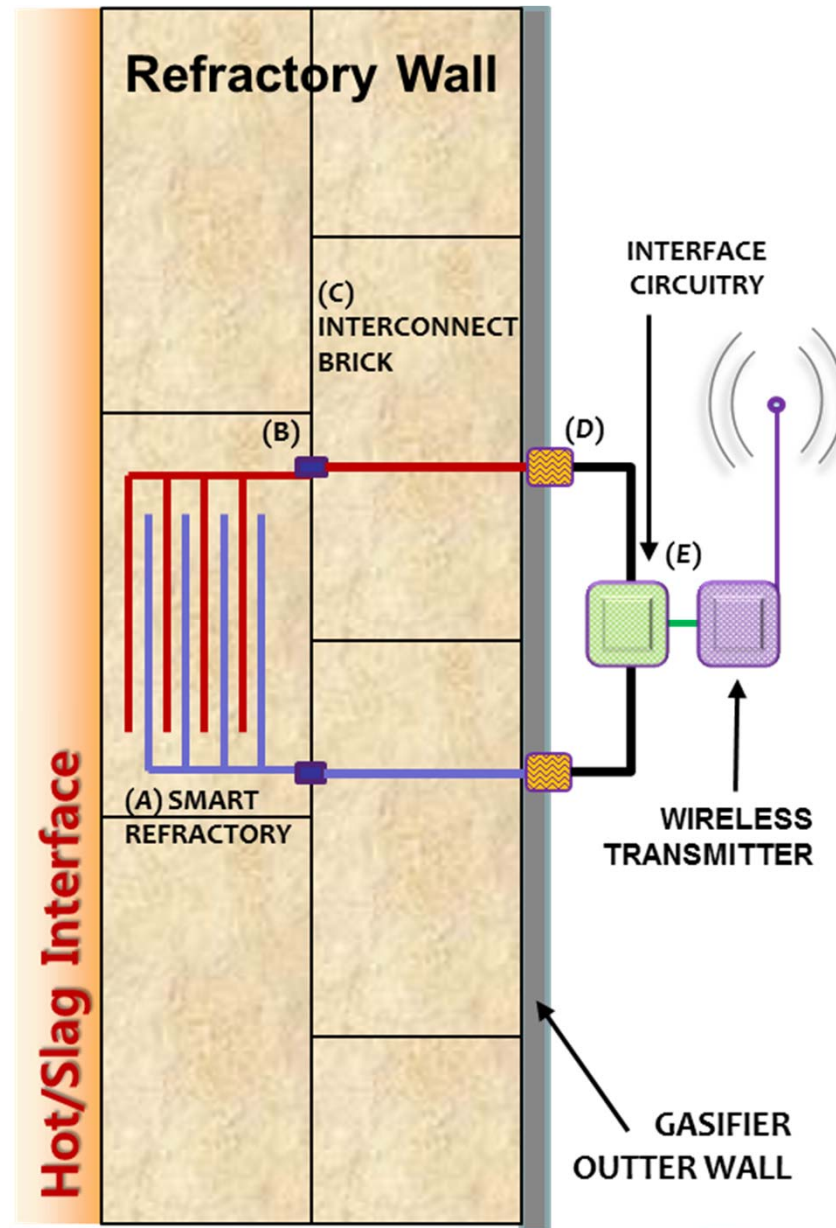
**Item A** represents the “smart refractory” material.

**Item B** is an interconnection (alignment) pin.

**Item C** is an interconnection brick, which will permit transfer of the signal to the exterior wall.

**Item D** is the sealed electrical access port to connect to the signal acquisition/processing units.

**Item E** is low-power electronics and wireless communication.



# *Program Objectives*

- 1) Investigate chemical stability, thermomechanical properties, and electrical properties of refractory ceramic composites at temperatures between 750-1450°C.
- 2) Define processes to pattern and embed the conductive ceramic composites within refractory materials to incorporate temperature and strain/stress sensors into refractory bricks.
- 3) Develop methods to interface the electrical sensing outputs from the smart refractory with an embedded processor and to design a wireless sensor network to efficiently collect the data at a processing unit for further data analysis.
- 4) Develop algorithms for model-based estimation of temperature profile in the refractory, slag penetration depth, spallation thickness, and resultant health by using the data from the wireless sensor network.



# *Task Assignments*

*Task 2: Fabrication and Characterization of Oxide-Silicide Composites.*

*Task 3 and Task 4: Sensor Patterning and Embedding and Static and Dynamic Sensor Testing.*

*Task 5: Data Ex-Filtration Using a Wireless Sensor Network.*

*Task 6: Model-Based Estimation of Refractory Degradation/Temperature.*



***Task 2:  
Fabrication and Characterization of  
Oxide-Silicide Composites.  
(Sabolsky)***



## ***Task 2.0 Objectives:***

- Investigate chemical stability, thermomechanical properties, and electrical properties of refractory silicide-oxide composites at temperatures between 750-1450°C.





# Silicide/Oxide Stability (XRD):

\* Prepared via mixed oxide route followed by sintering in Argon atmosphere at 1400°-1600°C.

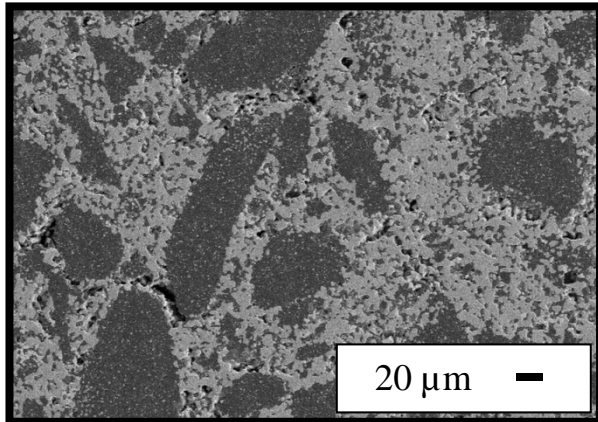
	Al <sub>2</sub> O <sub>3</sub>	Y <sub>2</sub> O <sub>3</sub>	ZrO <sub>2</sub>	Cr <sub>2</sub> O <sub>3</sub>
<b>MoSi<sub>2</sub></b>	MoSi <sub>2</sub> , Al <sub>2</sub> O <sub>3</sub> , SiO <sub>2</sub>	MoSi <sub>2</sub> , Y <sub>2</sub> O <sub>3</sub> , SiO <sub>2</sub> , Y <sub>5</sub> Mo <sub>2</sub> O <sub>12</sub> , Mo <sub>3</sub> Si, Mo <sub>3</sub> O	MoSi <sub>2</sub> , ZrO <sub>2</sub> , Mo <sub>5</sub> Si <sub>3</sub>	MoSi <sub>2</sub> , Cr <sub>2</sub> O <sub>3</sub> , Cr <sub>3</sub> Mo, SiO <sub>2</sub>
<b>WSi<sub>2</sub></b>	WSi <sub>2</sub> , Al <sub>2</sub> O <sub>3</sub> , W <sub>5</sub> Si <sub>3</sub>	WSi <sub>2</sub> , Y <sub>2</sub> SiO <sub>5</sub> , WO <sub>2</sub> , SiO <sub>2</sub>	WSi <sub>2</sub> , ZrO <sub>2</sub> , W <sub>5</sub> Si <sub>3</sub>	WSi <sub>2</sub> , Cr <sub>2</sub> O <sub>3</sub> , SiO <sub>2</sub> , W <sub>3</sub> O
<b>ZrSi<sub>2</sub></b>	ZrSi <sub>2</sub> , Al <sub>2</sub> O <sub>3</sub> , ZrO <sub>2</sub> , SiO <sub>2</sub>	ZrSi <sub>2</sub> , Y <sub>2</sub> O <sub>3</sub> , Y <sub>2</sub> Si <sub>2</sub> O <sub>7</sub> , SiO <sub>2</sub>	ZrSi <sub>2</sub> , ZrO <sub>2</sub> , SiO <sub>2</sub>	ZrSi <sub>2</sub> , Cr <sub>2</sub> O <sub>3</sub> , ZrSiO <sub>4</sub> , Cr <sub>3</sub> O, SiO <sub>2</sub>
<b>TaSi<sub>2</sub></b>	TaSi <sub>2</sub> , Al <sub>2</sub> O <sub>3</sub> , Ta <sub>5</sub> Si <sub>3</sub> , Ta <sub>3</sub> Si, SiO <sub>2</sub>	TaSi <sub>2</sub> , Y <sub>2</sub> SiO <sub>5</sub> , Ta <sub>2</sub> O <sub>5</sub> , Y <sub>10</sub> Ta <sub>4</sub> O <sub>25</sub>	TaSi <sub>2</sub> , ZrO <sub>2</sub> , Ta <sub>5</sub> Si <sub>3</sub> , SiO <sub>2</sub>	TaSi <sub>2</sub> , Cr <sub>2</sub> O <sub>3</sub> , CrTaO <sub>4</sub> , Ta <sub>2</sub> O <sub>5</sub> , TaO <sub>2</sub>
<b>NbSi<sub>2</sub></b>	NbSi <sub>2</sub> , Al <sub>2</sub> O <sub>3</sub> , Nb <sub>5</sub> Si <sub>3</sub>	NbSi <sub>2</sub> , Y <sub>2</sub> O <sub>3</sub> , Y <sub>2</sub> SiO <sub>5</sub> , Nb <sub>5</sub> Si <sub>3</sub> , SiO <sub>2</sub>	NbSi <sub>2</sub> , ZrO <sub>2</sub> , Nb <sub>5</sub> Si <sub>3</sub> , SiO <sub>2</sub>	NbSi <sub>2</sub> , Cr <sub>2</sub> O <sub>3</sub> , Nb <sub>5</sub> Si <sub>3</sub> , CrNbO <sub>4</sub> , CrNbSi, SiO <sub>2</sub>
<b>TiSi<sub>2</sub></b>	TiSi <sub>2</sub> , Al <sub>2</sub> O <sub>3</sub> , Ti <sub>5</sub> Si <sub>3</sub> , SiO <sub>2</sub>	TiSi <sub>2</sub> , Y <sub>2</sub> O <sub>3</sub> , Y <sub>2</sub> Si <sub>2</sub> O <sub>7</sub> , TiO <sub>2</sub> , SiO <sub>2</sub>	TiSi <sub>2</sub> , ZrO <sub>2</sub> , TiO <sub>2</sub> , SiO <sub>2</sub>	(Cr <sub>0.88</sub> Ti <sub>0.12</sub> ) <sub>2</sub> O <sub>3</sub> , Cr <sub>3</sub> Si, SiO <sub>2</sub>
<b>CrSi<sub>2</sub></b>	CrSi <sub>2</sub> , Al <sub>2</sub> O <sub>3</sub> , Cr <sub>5</sub> Si <sub>3</sub>	CrSi <sub>2</sub> , Y <sub>2</sub> O <sub>3</sub> , Y <sub>2</sub> SiO <sub>5</sub>	CrSi <sub>2</sub> , ZrO <sub>2</sub>	CrSi <sub>2</sub> , Cr <sub>2</sub> O <sub>3</sub> , Cr <sub>3</sub> Si, SiO <sub>2</sub>

- Metal silicides show high stability in Al<sub>2</sub>O<sub>3</sub> and ZrO<sub>2</sub> matrix only with formation of different type of silicides (Mo<sub>5</sub>Si<sub>3</sub>, W<sub>5</sub>Si<sub>3</sub>, Ta<sub>5</sub>Si<sub>3</sub>, Nb<sub>5</sub>Si<sub>3</sub>, Cr<sub>5</sub>Si<sub>3</sub>) and SiO<sub>2</sub> (highlighted).
- They partially react with Y<sub>2</sub>O<sub>3</sub> and Cr<sub>2</sub>O<sub>3</sub> to form undesired secondary phases.

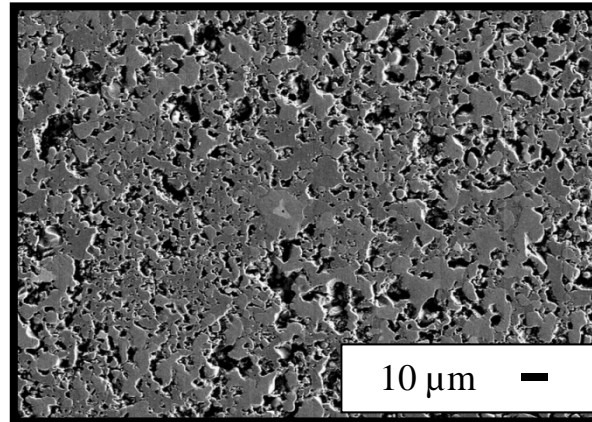


# Silicide/Oxide Microstructure (SEM):

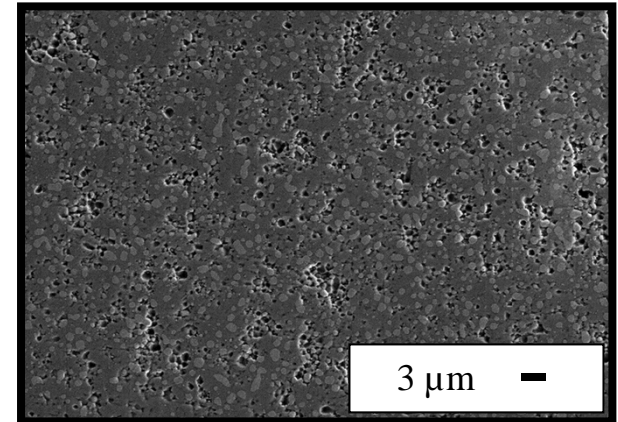
(60-40) vol% MoSi<sub>2</sub>-Al<sub>2</sub>O<sub>3</sub>



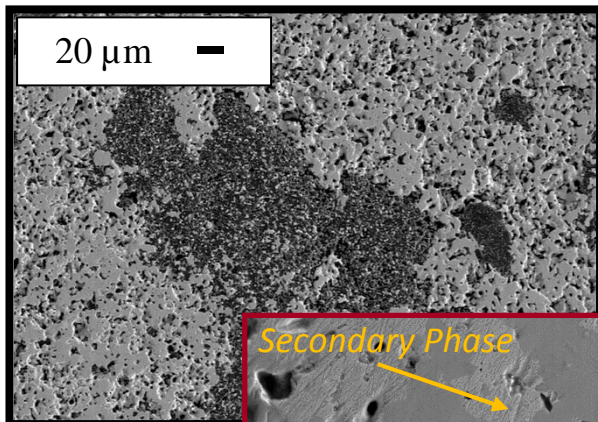
(60-40) vol% MoSi<sub>2</sub>-Y<sub>2</sub>O<sub>3</sub>



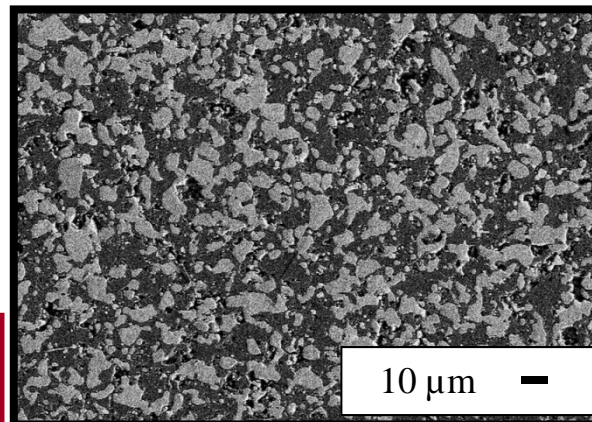
(60-40) vol% MoSi<sub>2</sub>-ZrO<sub>2</sub>



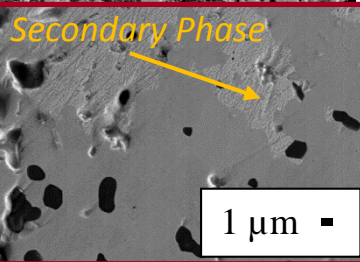
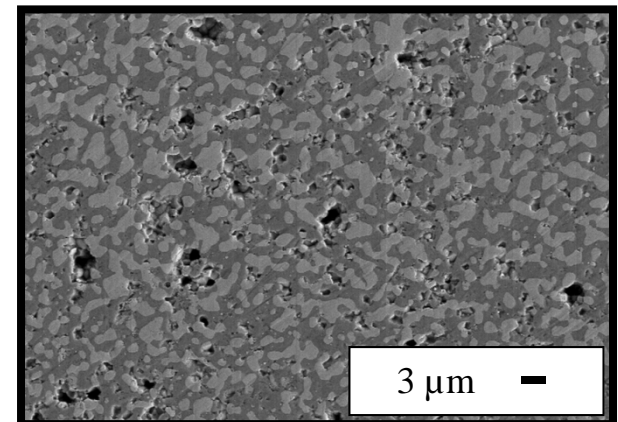
(60-40) vol% WSi<sub>2</sub>-Al<sub>2</sub>O<sub>3</sub>



(60-40) vol% WSi<sub>2</sub>-Y<sub>2</sub>O<sub>3</sub>



(60-40) vol% WSi<sub>2</sub>-ZrO<sub>2</sub>

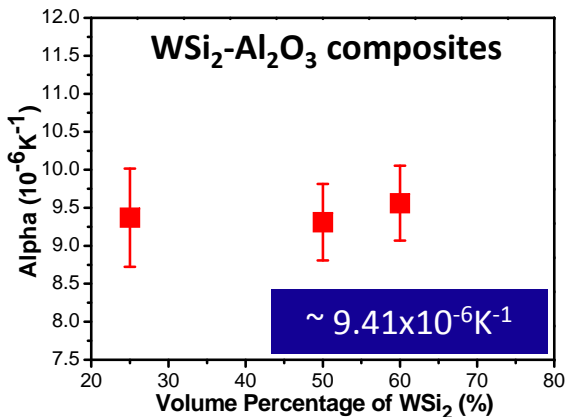
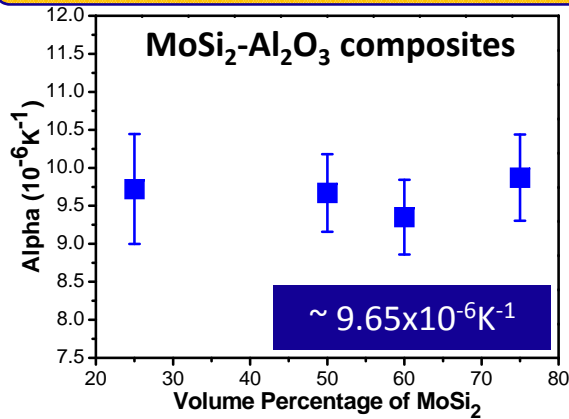


Chemically etched in 1:1:1 HCl:HNO<sub>3</sub>:H<sub>2</sub>O

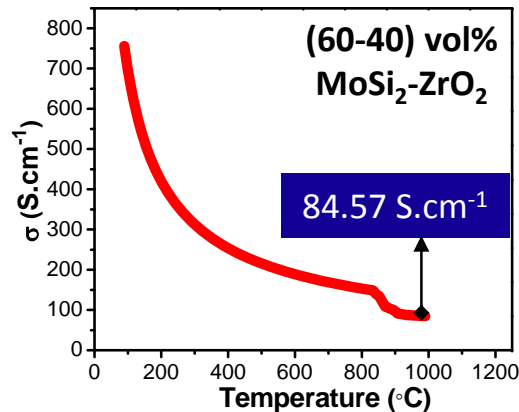
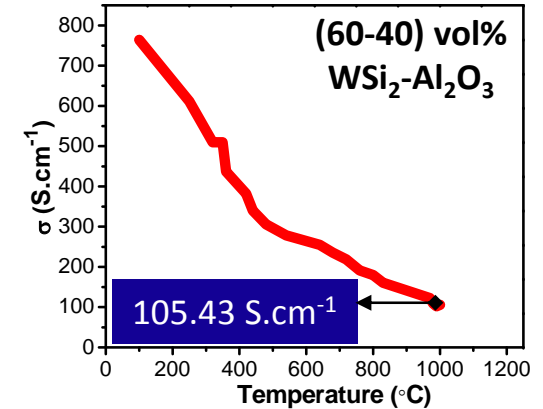
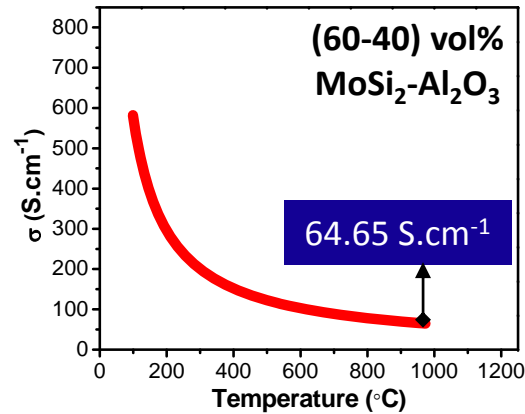


# Silicide/Oxide Properties:

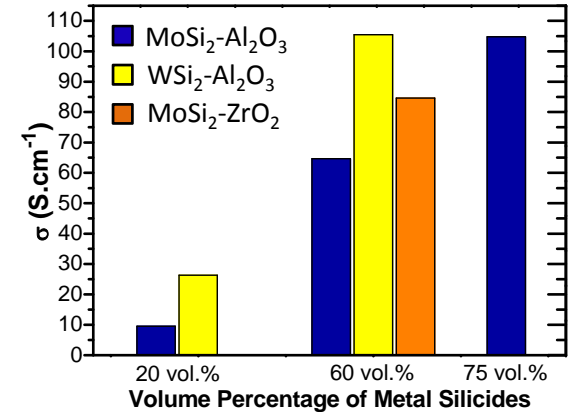
## CTE (100°-1000°C)



## 4-point DC Conductivity (100°-1200°C)



## Electrical Conductivities at 1000°C



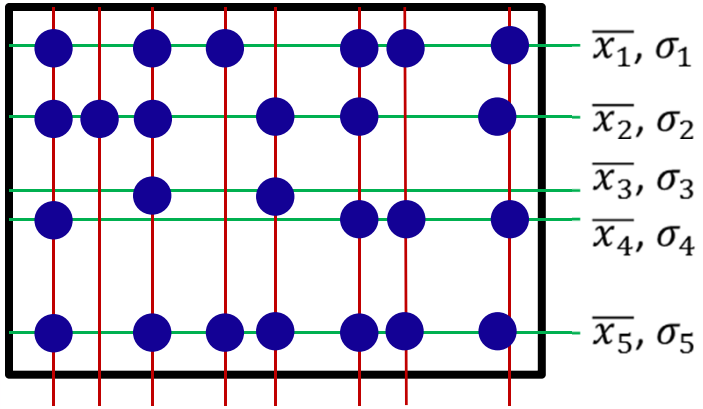
- Electrical conductivity of composites increases with increasing metal silicide volume fraction (0.2 to 0.75) while it decreases with increasing temperature (100° to 1200°C).

• **Key Parameters:** Distribution of metal silicides within refractory ceramic matrix, and density.



# Image Analysis for Distribution (SEM):

**Proposed Methods:** Determination of standard deviation and coefficient of variation by measuring distances between all neighboring silicide grains via ImageJ



**Method #1**

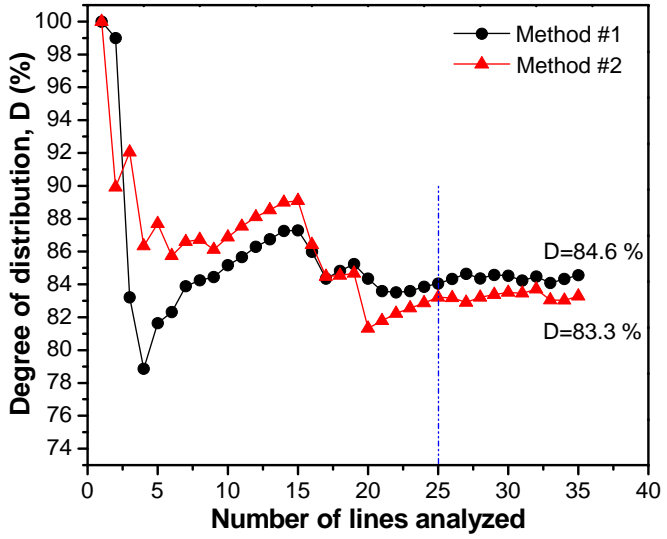
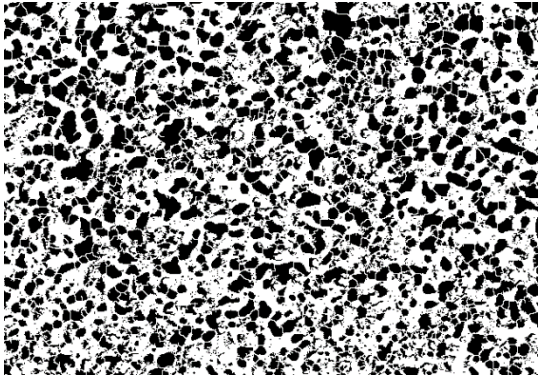
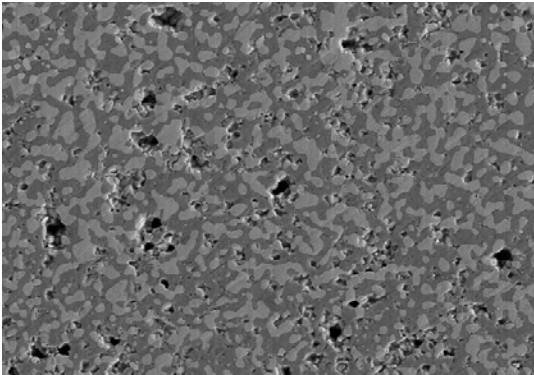
$$D = 100 - \left( \frac{\text{standard deviation of } \bar{x}_1, \bar{x}_2, \bar{x}_3, \dots}{\text{mean of } \bar{x}_1, \bar{x}_2, \bar{x}_3, \dots} \right) \times 100$$

**Method #2**

$$D = 100 - \left( \frac{\text{standard deviation of } \sigma_1, \sigma_2, \sigma_3, \dots}{\text{mean of } \sigma_1, \sigma_2, \sigma_3, \dots} \right) \times 100$$

D = degree of distribution (mixedness)

(60-40) vol% WSi<sub>2</sub>-ZrO<sub>2</sub>



Original image → Binary image

$\bar{x}_n$  = average distance btw grains;  $n$  = number of lines analyzed;  $\sigma_n$  = standard deviation;



## ***Task 2 Conclusions and Future Work:***

- Metal silicides show high stability in  $\text{Al}_2\text{O}_3$  and  $\text{ZrO}_2$  matrix only with formation of different type of silicides such as  $\text{Mo}_5\text{Si}_3$ ,  $\text{W}_5\text{Si}_3$ ,  $\text{Ta}_5\text{Si}_3$ ,  $\text{Nb}_5\text{Si}_3$ ,  $\text{Cr}_5\text{Si}_3$  and  $\text{SiO}_2$ .
- Electrical conductivity of composites increases with increasing metal silicide volume fraction (0.2 to 0.75) while it decreases with increasing temperature (100 to 1200 °C).

### ***Future Work:***

- Alternative materials and designs (layered structure...) will be investigated to prevent the reaction between silicide/oxide composites and  $\text{Cr}_2\text{O}_3$ .
- Image analysis on SEM micrographs will be performed to characterize degree of distribution (mixedness) in order to find its effect on properties (conductivity...) and to optimize process parameters.



***Task 3: Sensor Patterning and  
Embedding.(Sabolsky/Palmisiano)***

***Task 4: Static and Dynamic Sensor Testing  
of Smart Refractory Specimens.  
(Sabolsky)***



\*US Provisional Patent Number 61/941,159



## ***Task 3 Objectives:***

- To develop methods for patterning technology the ceramic composites within the refractory matrix.
- To engineer the powder properties and thermal processing to successfully incorporate the sensor structures within the refractory.

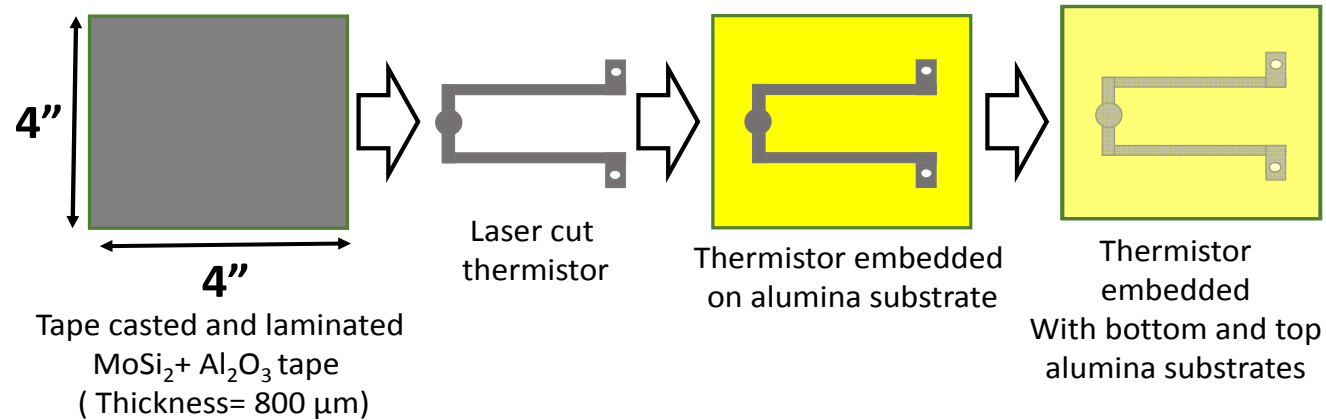
## ***Task 4 Objectives:***

- To investigate corrosion/erosion kinetics in static and dynamic tests on smaller prototype and full-size smart cups and bricks (at WVU and HWI).
- To implement and test methods for data collection on initial prototypes.

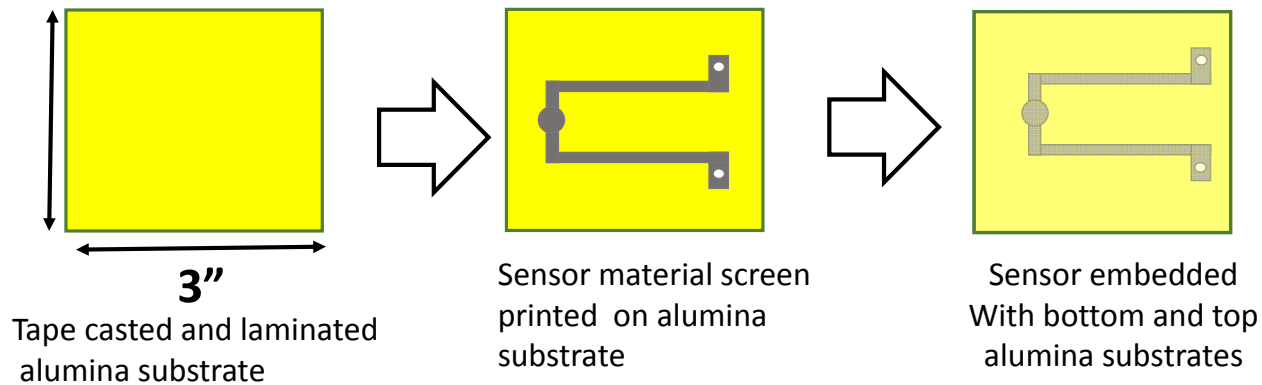


# Sensor Preform Fabrication:

## 1. Fabrication of sensor through tape casting

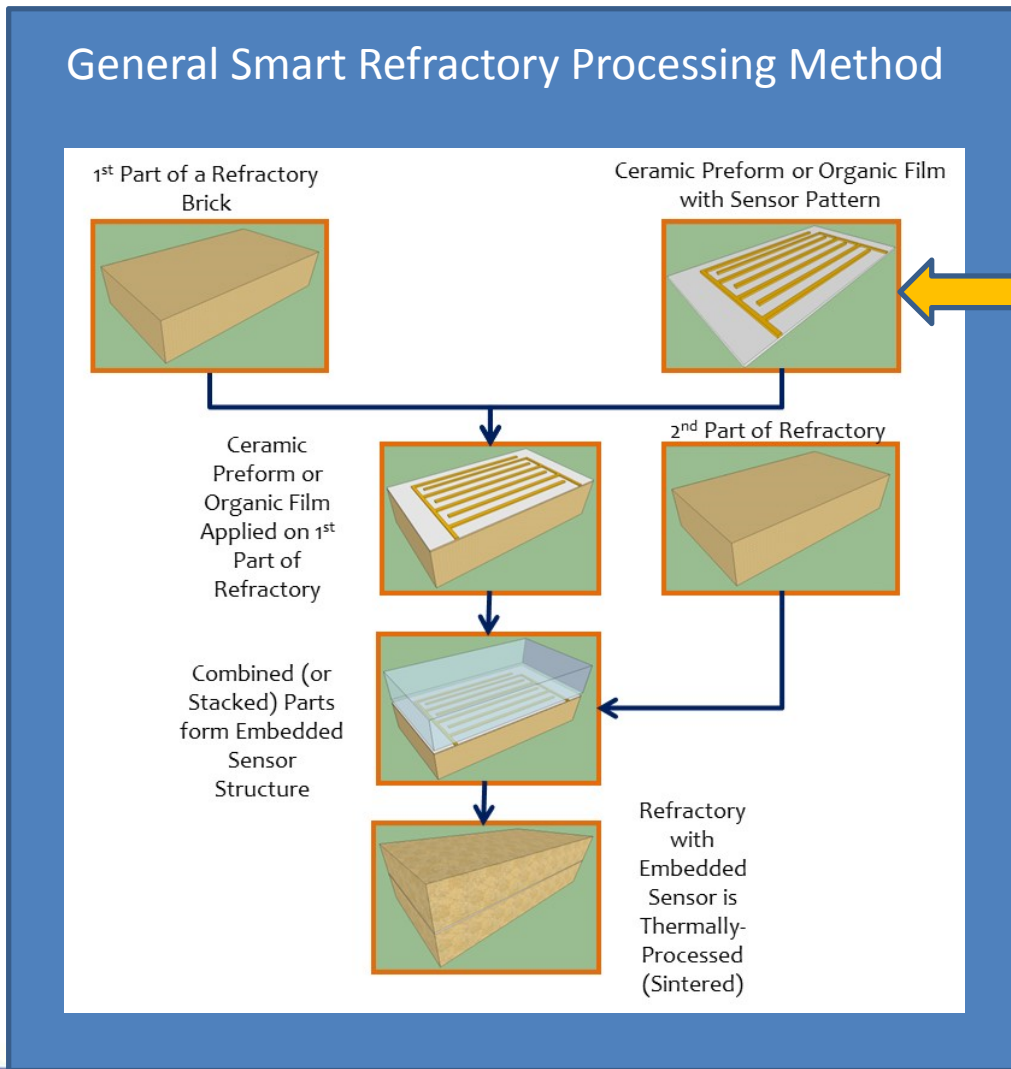


## 2. Fabrication of sensor through screen printing

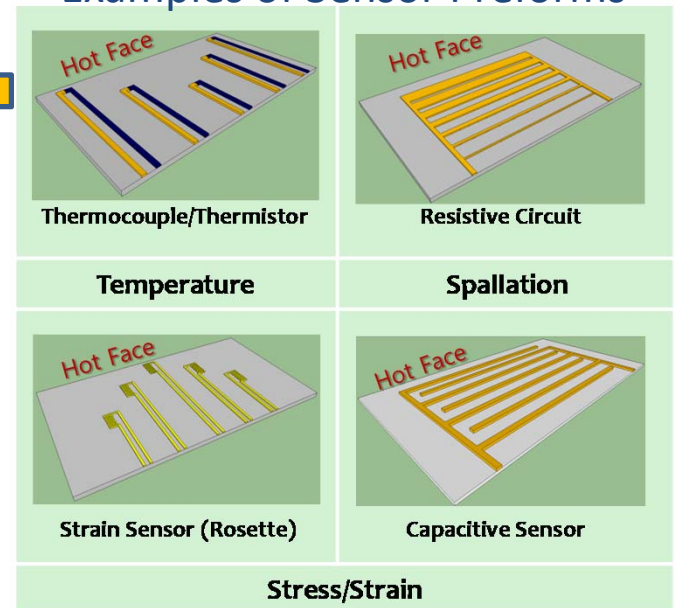




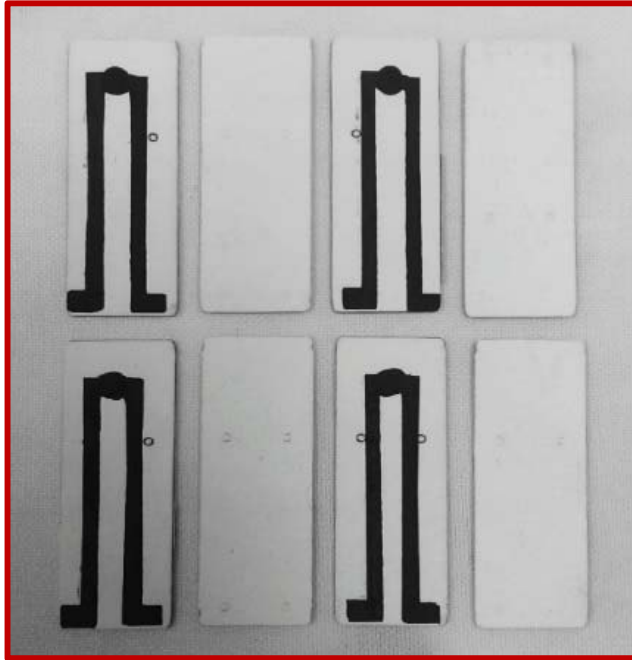
# Smart Refractory Fabrication:



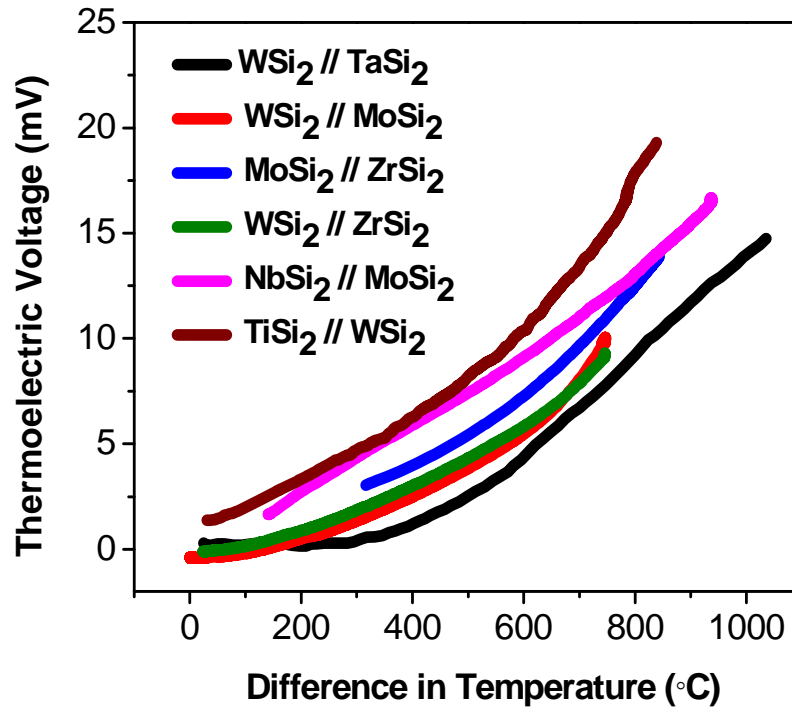
## Examples of Sensor Preforms



# Ceramic Thermocouple Performance: (High-temperature measurements)



Preforms and laminated forms of ceramic thermocouples heated at 1500 °C and performance is evaluated at 1000 °C.

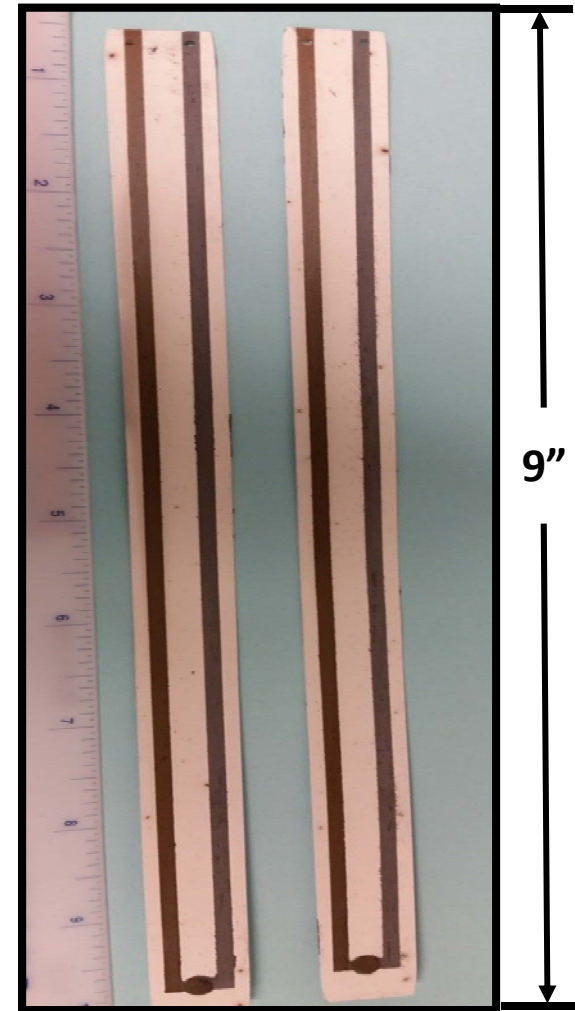
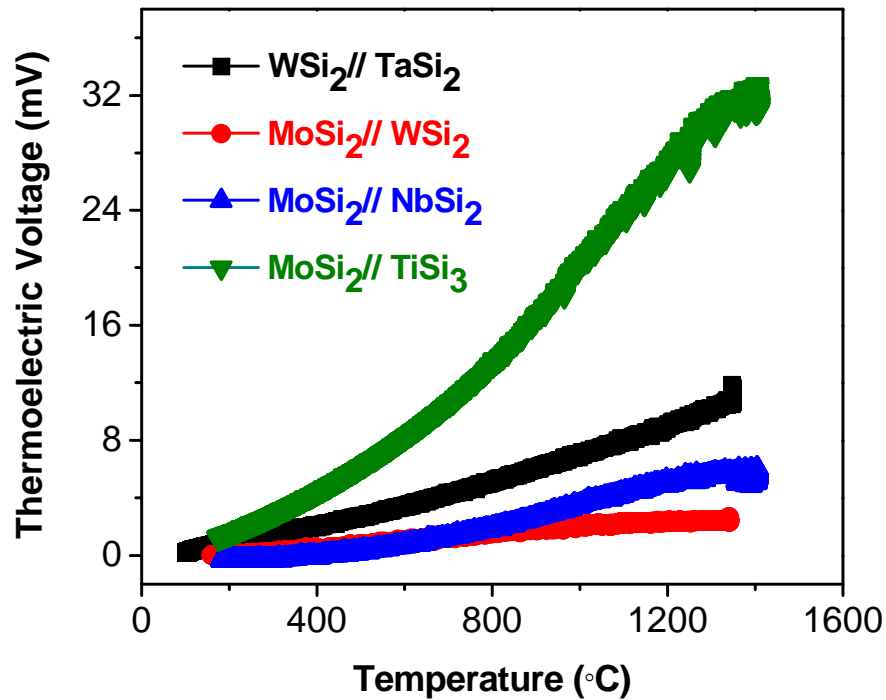


1. [90-10]WSi<sub>2</sub>-Al<sub>2</sub>O<sub>3</sub>//[90-10]TaSi<sub>2</sub>-Al<sub>2</sub>O<sub>3</sub>
2. [90-10]WSi<sub>2</sub>-Al<sub>2</sub>O<sub>3</sub>//[90-10] MoSi<sub>2</sub>-Al<sub>2</sub>O<sub>3</sub>
3. [90-10]MoSi<sub>2</sub>-Al<sub>2</sub>O<sub>3</sub>//[90-10] ZrSi<sub>2</sub>-Al<sub>2</sub>O<sub>3</sub>
4. [90-10]WSi<sub>2</sub>-Al<sub>2</sub>O<sub>3</sub>// [90-10] ZrSi<sub>2</sub>-Al<sub>2</sub>O<sub>3</sub>
5. [90-10]NbSi<sub>2</sub>-Al<sub>2</sub>O<sub>3</sub>//[90-10] MoSi<sub>2</sub>-Al<sub>2</sub>O<sub>3</sub>
6. [90-10] TiSi<sub>2</sub>-Al<sub>2</sub>O<sub>3</sub>//[90-10] WSi<sub>2</sub>-Al<sub>2</sub>O<sub>3</sub>

**TiSi<sub>2</sub>// WSi<sub>2</sub> exhibited 20 mV at 800 °C  
(Type B= 3.15 mV at 800°C)**



# High-Temperature Thermocouple Performance:



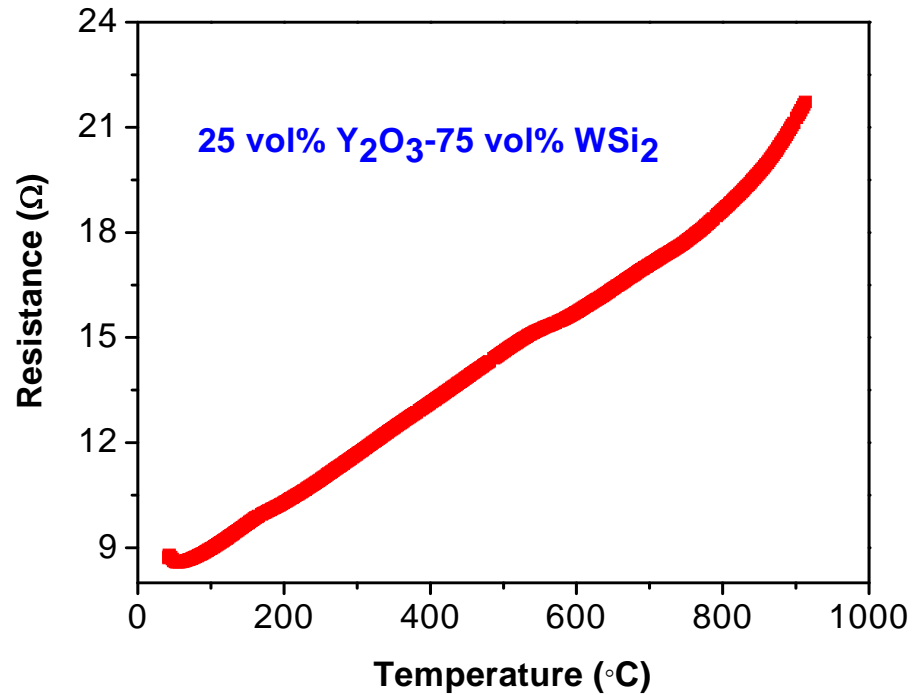
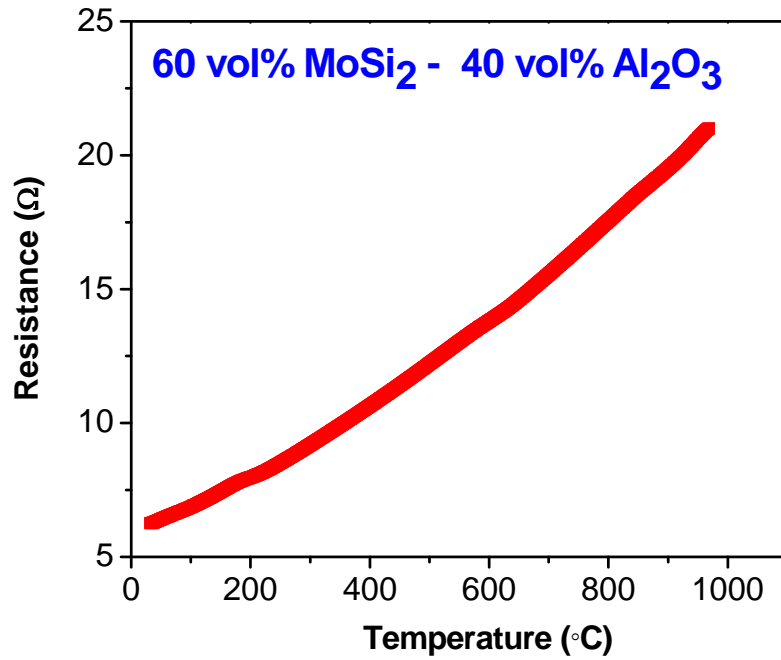
Various thermocouple compositions studied at 1500 °C →

1. [90-10]WSi<sub>2</sub>-Al<sub>2</sub>O<sub>3</sub>//[90-10]TaSi<sub>2</sub>-Al<sub>2</sub>O<sub>3</sub>
2. [90-10]MoSi<sub>2</sub>-Al<sub>2</sub>O<sub>3</sub>//[90-10]WSi<sub>2</sub>-Al<sub>2</sub>O<sub>3</sub>
3. [90-10]MoSi<sub>2</sub>-Al<sub>2</sub>O<sub>3</sub>//[90-10]NbSi<sub>2</sub>-Al<sub>2</sub>O<sub>3</sub>
4. [90-10]MoSi<sub>2</sub>-Al<sub>2</sub>O<sub>3</sub>//[90-10]TiSi<sub>2</sub>-Al<sub>2</sub>O<sub>3</sub>



The thermocouple with composition MoSi<sub>2</sub>//TiSi<sub>2</sub> exhibited 34 mV at 1400 °C

# Thermistor Performance:



Composition studied:

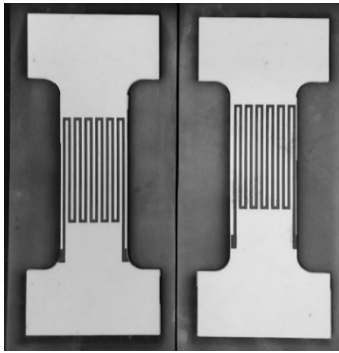
1. [40-60] MoSi<sub>2</sub>-Al<sub>2</sub>O<sub>3</sub>
2. [60-40] MoSi<sub>2</sub>-Al<sub>2</sub>O<sub>3</sub>
3. [75-25] MoSi<sub>2</sub>-Al<sub>2</sub>O<sub>3</sub>
4. [50-50] MoSi<sub>2</sub>-Al<sub>2</sub>O<sub>3</sub>
5. [25-40] WSi<sub>2</sub>-Y<sub>2</sub>O<sub>3</sub>

The increase of MoSi<sub>2</sub> in alumina matrix decreases the resistance of the thermistor

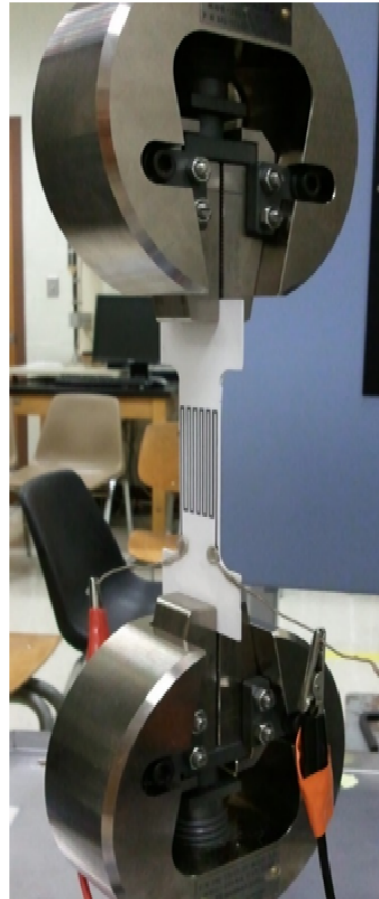
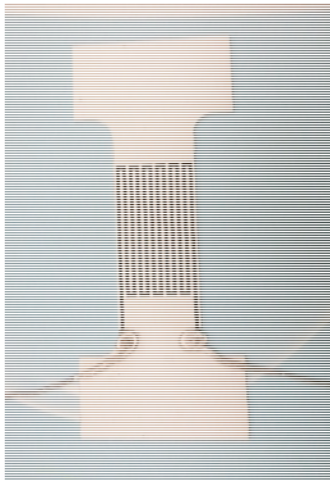


# Performance: Initial Strain Sensor Testing

Design #2

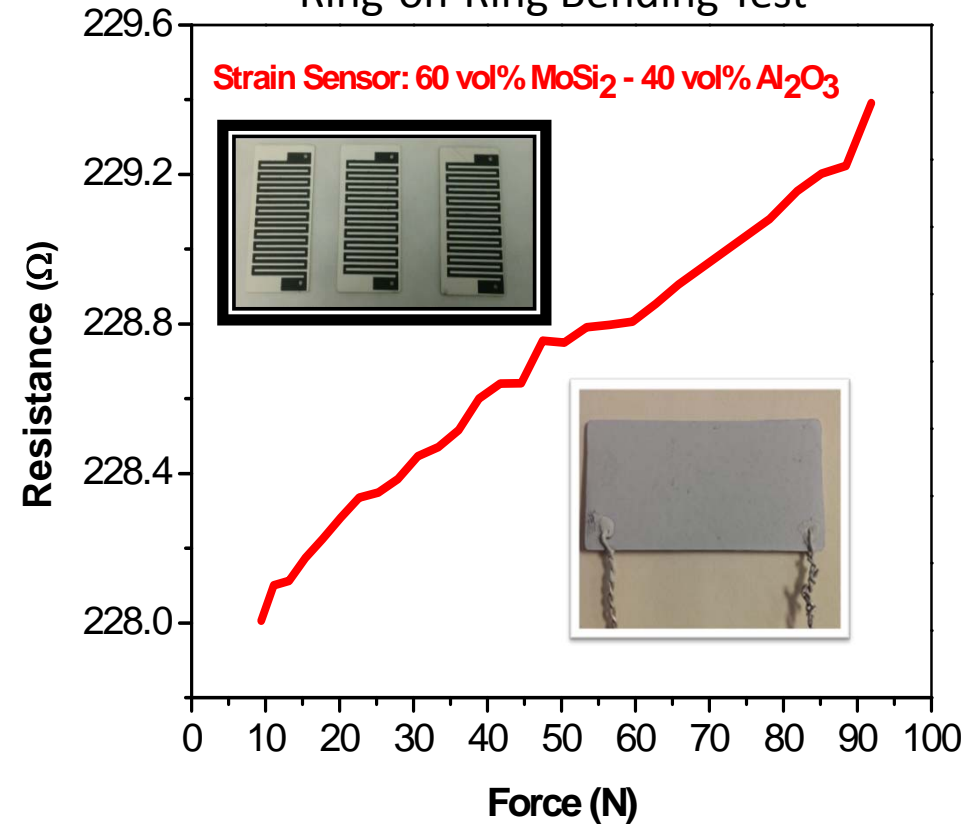


Design #2 wired



Tensile test using Instron

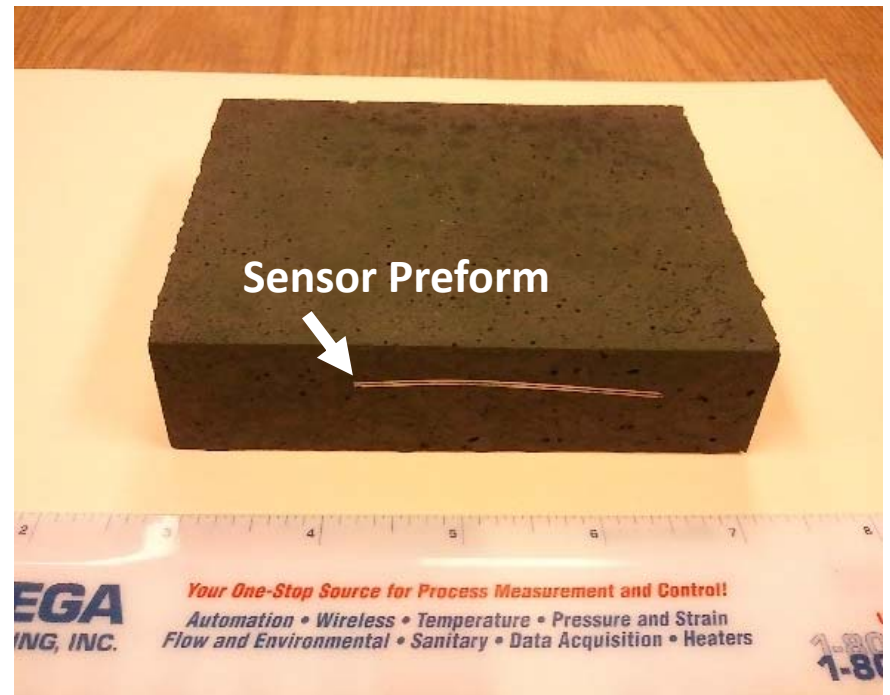
Ring-on-Ring Bending Test



# Smart Refractory Demonstrations:



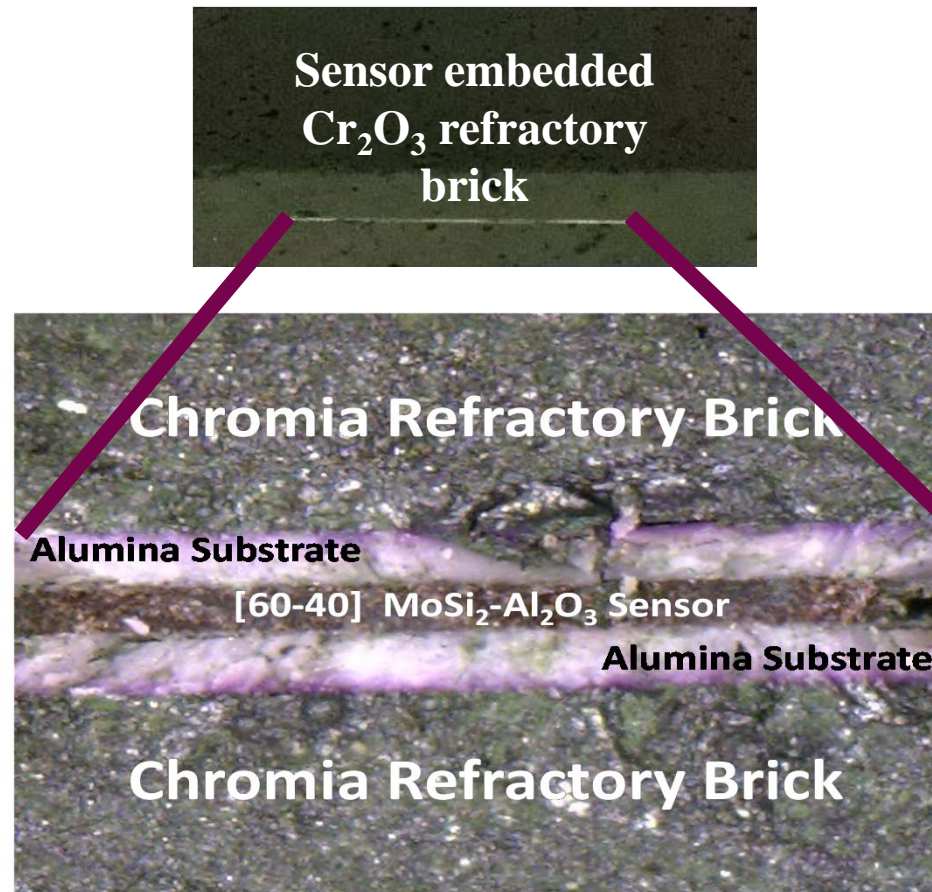
Fired high-chromia brick with sensor (thermistor).



The cut away portion of the fired brick showing the embedded sensor (thermistor).



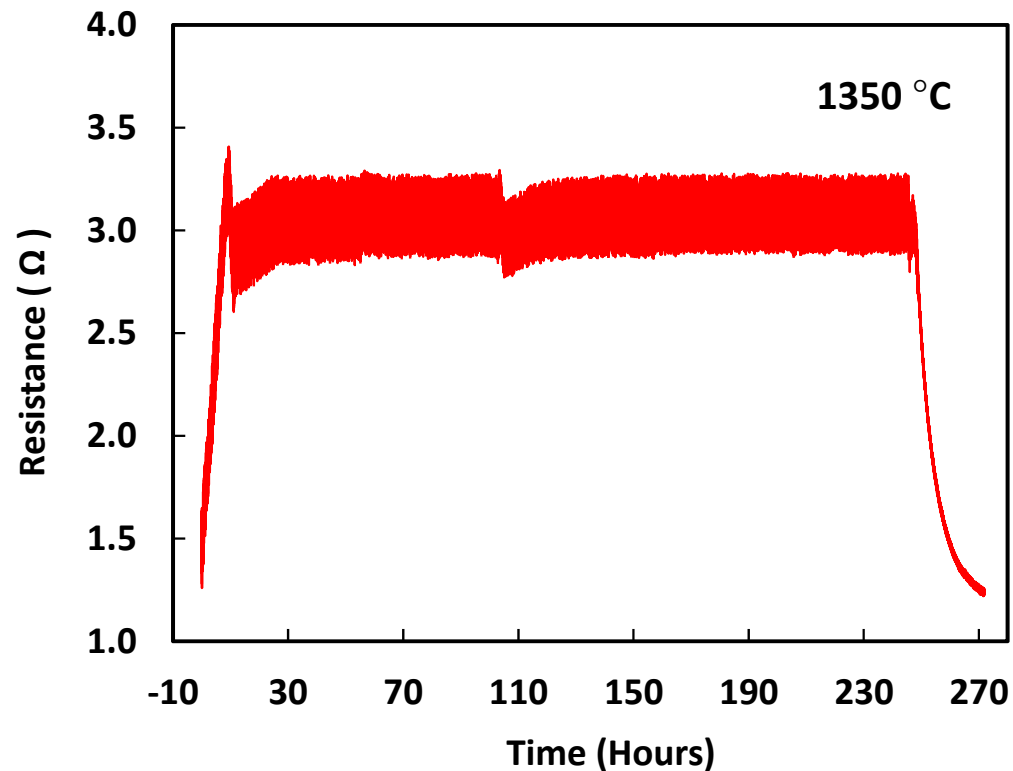
# Smart Refractory Microstructure:



Monoliths of sensors were fabricated via tape casting, laminated and sintered at 1500 °C. These laminates were embedded in the Cr<sub>2</sub>O<sub>3</sub> brick while slip casting and co-sintered at 1500° C in Argon atmosphere.



# Smart Refractory Performance:



Chromia brick showing exposed sensor preform.

The temperature sensor (thermistor) with composition (60-40) vol%  $\text{MoSi}_2\text{-Al}_2\text{O}_3$  embedded within the  $\text{Cr}_2\text{O}_3$  refractory exhibited stable behavior for more than 250 hours at 1350 °C in argon atmosphere.





# ***Task 3 and 4 Conclusions and Future Work:***

- Sensor preforms for various sensor architectures were using various silicide-oxide composites.
- Methods were developed to embed and test sensor preforms into high-chromia refractory.

## ***Future Work:***

- Optimize the composition to achieve maximum thermoelectric voltage of ceramic-ceramic thermocouples.
- Embed the thermocouples into the refractory bricks and evaluate the thermal, mechanical stability.
- Investigate the corrosion/erosion kinetics of sensor embedded refractory bricks in static and dynamic mode with slag.



***Task 5:  
Data Ex-Filtration Using a Wireless  
Sensor Network.  
(Graham/Kulathumani)***



## *Task 5 Objectives:*

- To develop methods to interface the electrical sensing outputs from the smart refractory with an embedded processor
- To design a wireless sensor network to efficiently collect the data at a processing unit for further data analysis



# *Electronics interfacing – Approach*

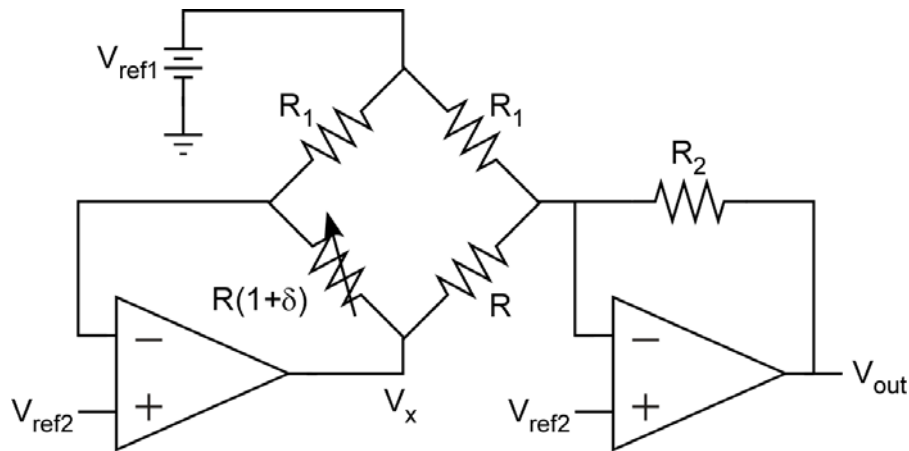
**Aim:** To reliably collect data from the sensors embedded within the smart bricks and interface them to wireless sensor nodes for communication

## **Approach:**

- (i) Iterative approach to sensor interface circuitry in parallel with the sensor development
  - a) Initial sensor interface circuitry using off-the-shelf circuitry
  - b) Move to integrated circuits for lower-power and more compact solutions
- (ii) Investigate energy harvesting using thermoelectric devices to help power the sensor motes and interface circuitry (*starts in year 2*)

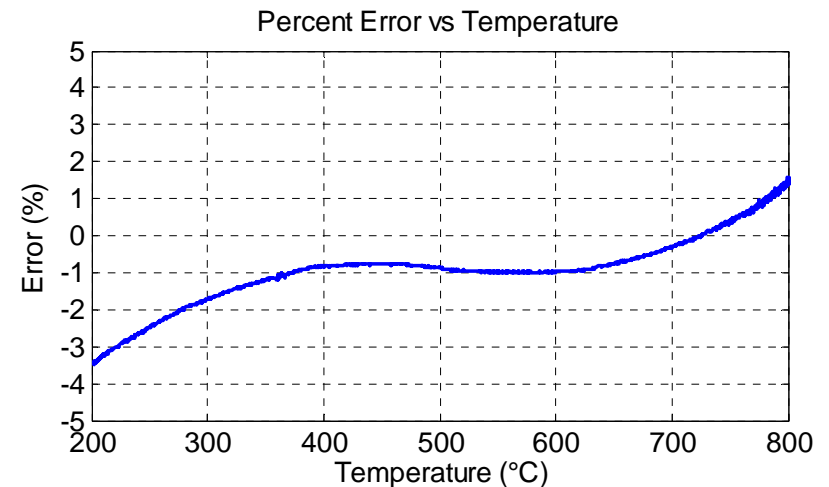
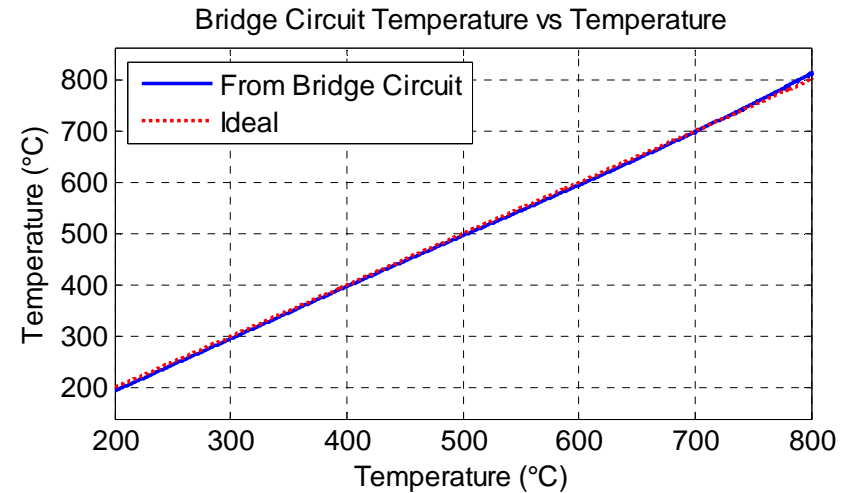


# Circuits for Resistor-Based Sensors

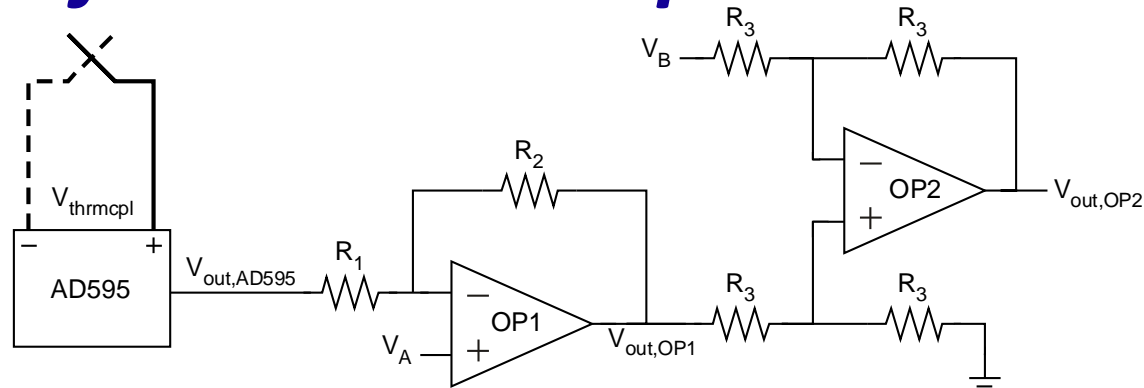


$$V_{out} = V_{ref2} + \frac{R_2}{R_1} \delta (V_{ref1} - V_{ref2})$$

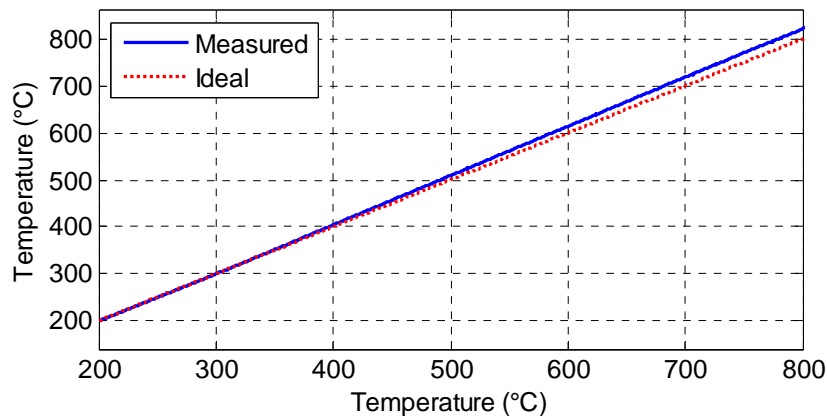
- Based on Wheatstone bridge
- Relatively low power (only 2 amps, no instrumentation amp)
- Linearizes the sensor output
- Single rail operation
- Easily adjusted parameters
  - $R_1$ ,  $R_2$ , and  $V_{ref1}$  set temperature range [ $T_{min}$  to  $T_{max}$ ]
  - $R$  sets temperature range median
- Easily modifiable for developing / improving sensors



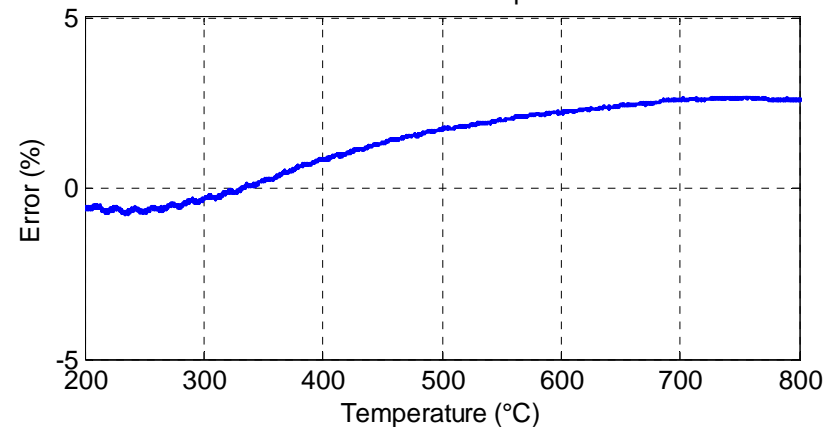
# Circuits for Thermocouple-Based Sensors



Circuit Measurement vs Ideal Temperature



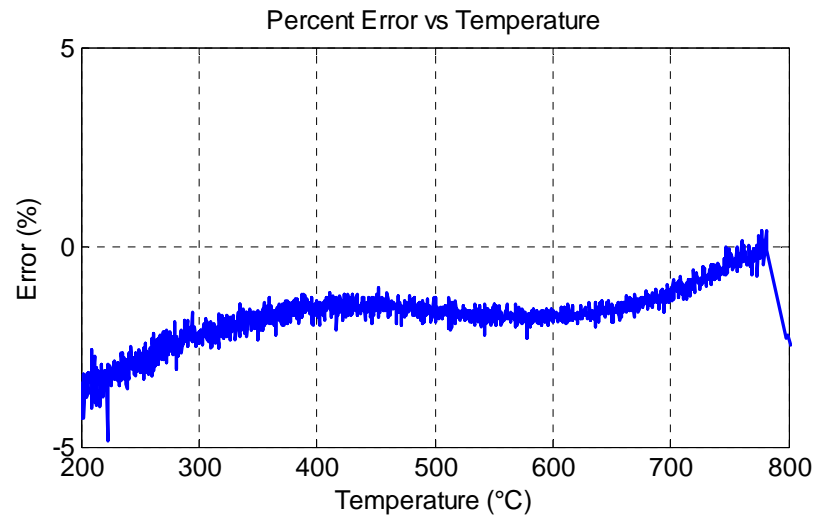
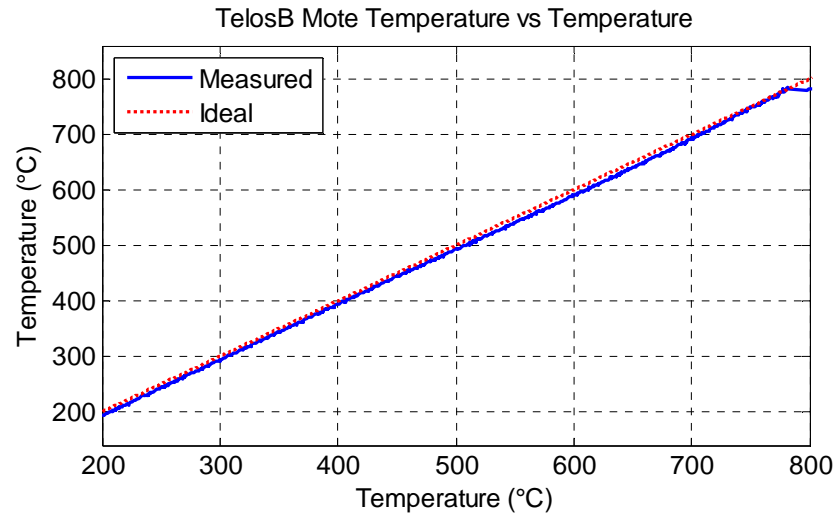
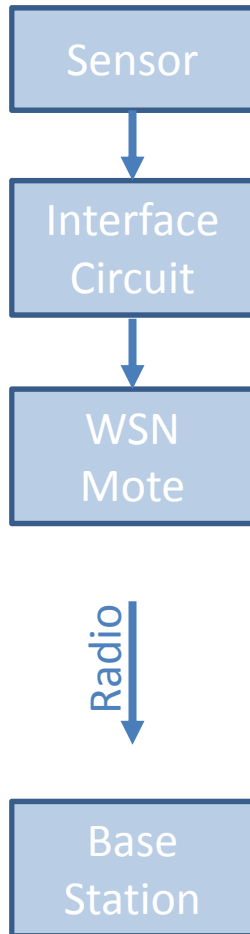
Percent Error vs Temperature



- Leverages COTS-based thermocouple circuit
  - AD595 provides appropriate amplification and cold-junction compensation
  - Single rail operation
  - Analog voltage output
- Remainder circuits adjust output reading to levels appropriate for WSN mote
- Verified with commercially available K-type thermocouple



# Interfacing with Wireless Sensor Nodes



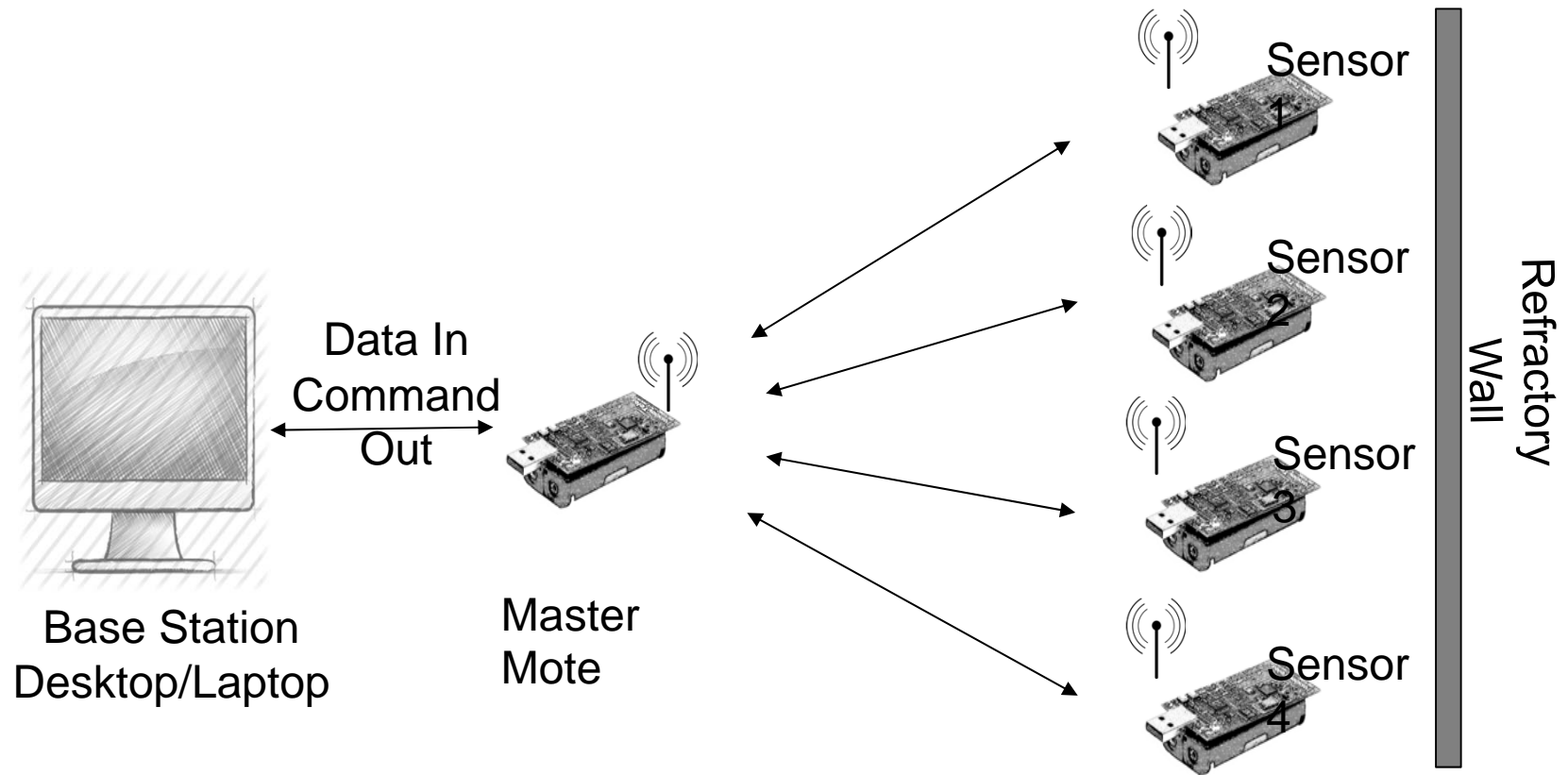
# Future Work

- (i) Continue improvement of sensor interface circuits
  - a) Interface with the new custom sensors being developed for this project and adjust as needed
  
- (ii) Investigation of thermoelectric devices for energy harvesting
  - a) Use off-the-shelf thermoelectric devices
  - b) Create energy transfer circuitry
  - c) Investigation of energy harvesting to supplement battery power within this application
  
- (iii) Integrated circuit development for lower-power operation
  - a) Complete the fast and accurate programming circuitry for in-the-field parameter adjustment
  - b) Translate sensor interface circuitry to integrated-circuit implementations



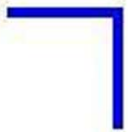


# Wireless sensor network overview



- Collect refractory sensor data over wireless medium (data ex-filtration)
- Enable remote configuration of parameters (over-the-air programming)



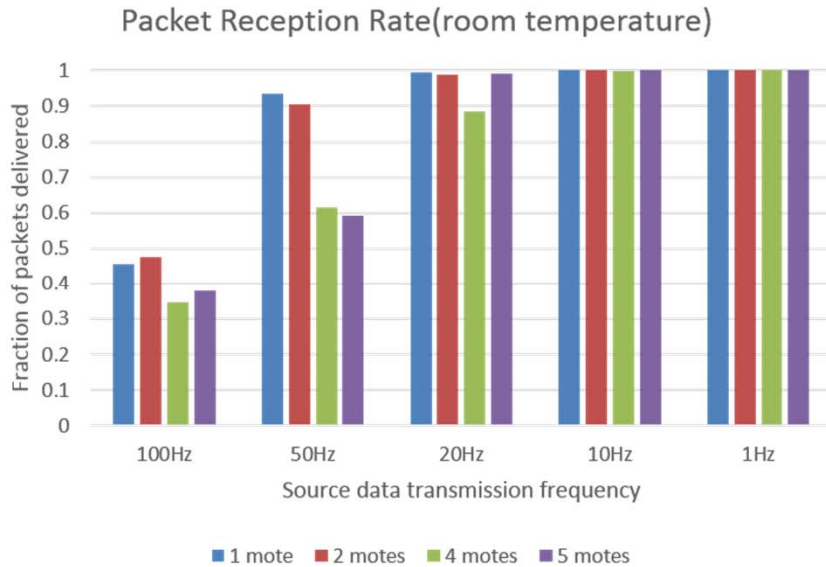


## ***Task Status:***

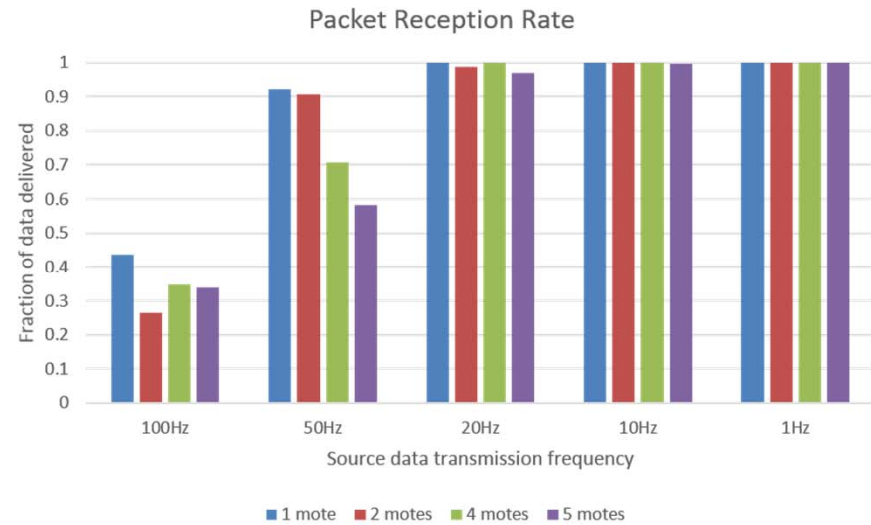
- Code for interfacing mote (radio + microcontroller) with the sensor circuits has been designed and tested
- Network protocol for collection of data at the base station has been implemented and tested
- On the go parameter change has been implemented.
  - The base station sends data to a master mote on UART and the master broadcasts the commands wirelessly to the sensor motes
  - Sampling intervals and broadcast rates can be changed dynamically
- The wireless system has been tested inside the furnace setup in lab to estimate link quality and packet loss.
- A user friendly Graphical Interface has been designed for data visualization and on the go parameter change.



# Testing Data Collection Performance:



Percentage of packets received at the base station as a function of network size and source data transmission frequency (room temperature; no furnace)

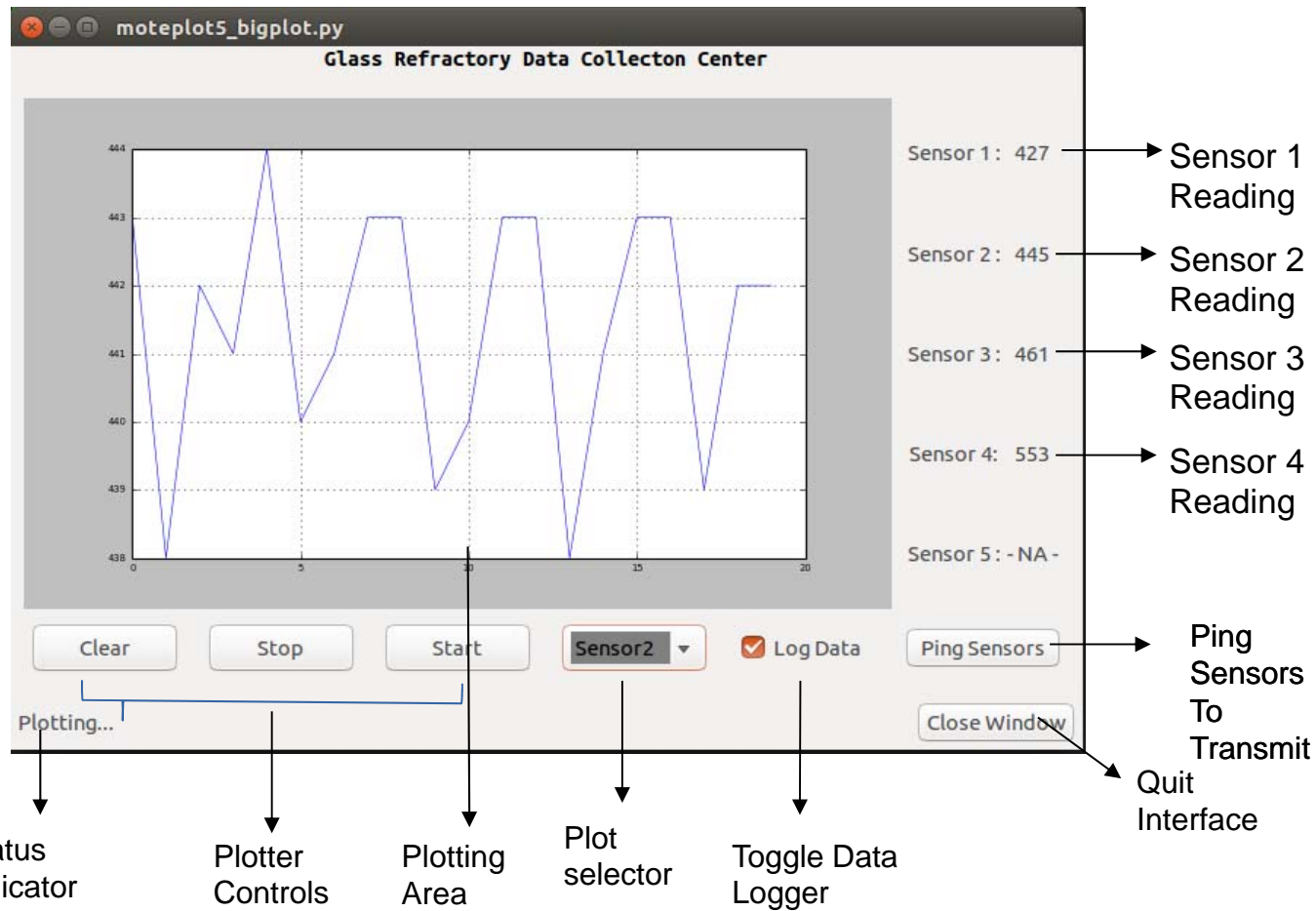


Percentage of packets received at the base station as a function of network size and source data transmission frequency (outside furnace at 1400c, inside an enclosed chamber)

Testing data collection performance over wireless network, with and without furnace; 1Hz – 20Hz are reasonable operating regions for refractory monitoring and high packet reception rates are observed in this range; No significant deterioration observed when operating near hot furnace



# Graphical User Interface for Visualizing and Control:



The GUI is able to show sensor signals in real time and also control individual sensor parameters such as sampling frequency and data transmission rate



## *Task 5 Conclusions and Future Work:*

- The end to end data collection system has been implemented and tested using simulated sensor signals
  - Sensors are interfaced with microcontroller + radio (motes)
  - Data collection protocol has been implemented
  - Visualization and sensor control interfaces have been implemented
- The next step is to test this system inside a real operating environment
- Possibility for model based data reduction techniques are being explored
  - This can help reduce data rate without compromising with information required for analyzing the system.



***Task 6.0:***  
***Model-Based Estimation of***  
***Temperature Profile and Extent of***  
***Refractory Degradation.***  
**(Bhattacharyya)**



## *Task 6 Objectives:*

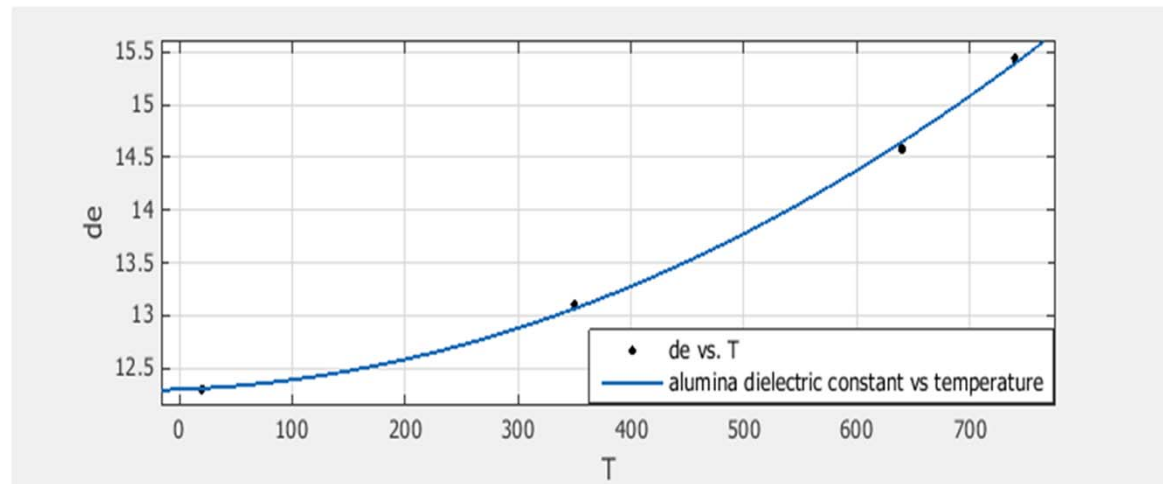
- To develop algorithms for model-based estimation of temperature profile in the refractory, slag penetration depth, spallation thickness, and resultant health by using the data from the wireless sensor network



# Property Models:

In order to build the model of smart refractory , several temperature-dependent property models for refractory and sensor material are needed:

- ❖ Specific heat
- ❖ Emissivity
- ❖ Thermal conductivity
- ❖ Electrical conductivity
- ❖ Thermal expansion
- ❖ Dielectric constant
- ❖ Young's modulus
- ❖ Poisson's ratio



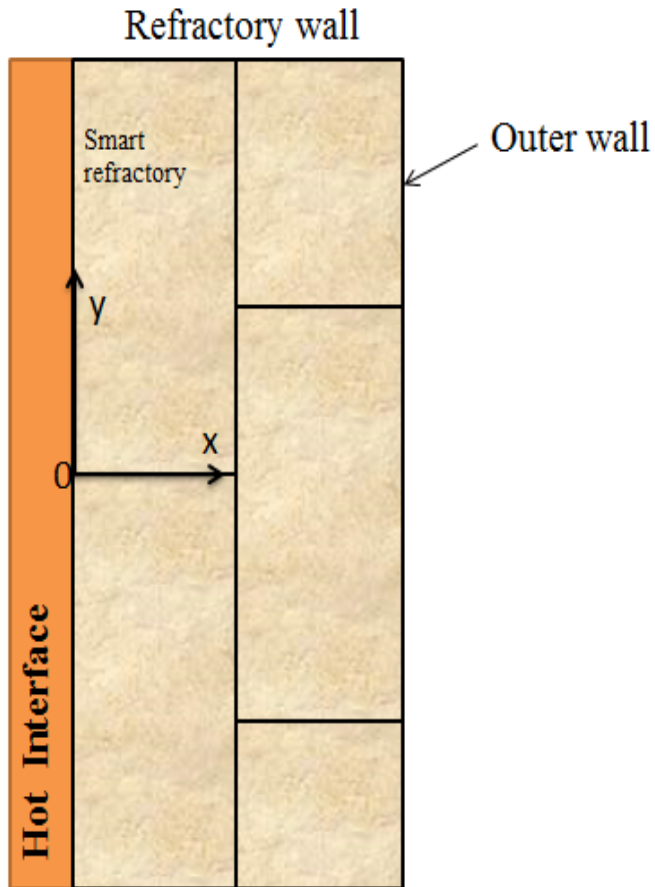
$$\epsilon = 5.098 \times 10^{-6} T^2 + 0.000406 \times T + 12.3 \text{ T in } ^\circ\text{C}$$

\* Data from: Birdsell E D, Park J, Allen M G. Wireless ceramic sensors operating in high temperature environments, 40th AIAA/ASME/SAE/ASEE Joint Propulsion Conference. 2004





# Thermal Model of the Refractory Brick:



- The thermal model is necessary for the proposed model based approach.

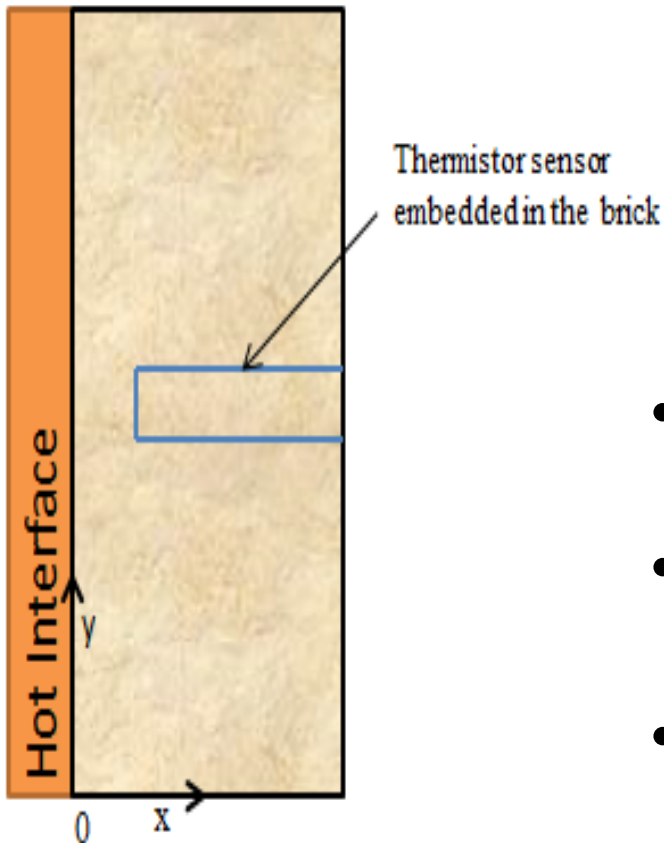
- 2-D heat conduct model:

$$\frac{\partial T}{\partial t} = \frac{K}{\rho C_P} \left( \frac{\partial^2 T}{\partial x^2} + \frac{\partial^2 T}{\partial y^2} \right)$$

- Two-dimensional model was developed in Aspen Custom Modeler<sup>®</sup> (ACM).



# Thermistor-type Sensor Model:



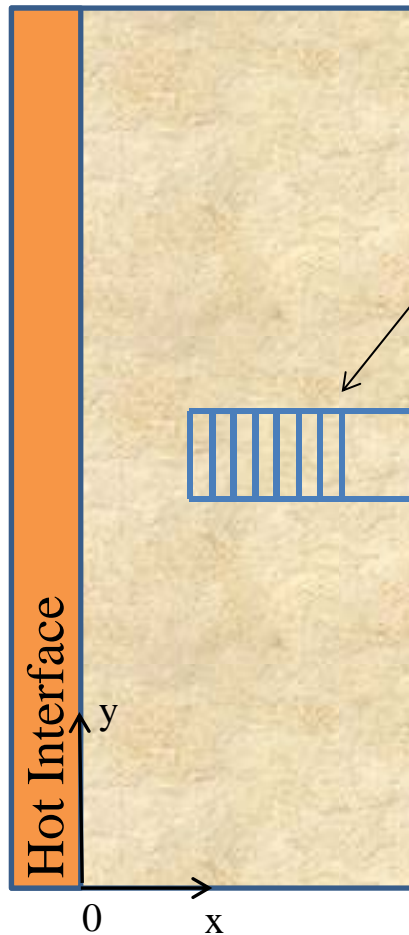
- The resistance of the thermistor can change significantly as a result of the temperature.

$$\sigma_x \frac{\partial^2 \phi}{\partial x^2} + \sigma_y \frac{\partial^2 \phi}{\partial y^2} = 0$$

- Significant temperature gradient can exist along the length of the thermistor.
- Slag penetration affects the temperature gradient
- Spatial distribution of sensors accounted for in the model



# Resistive Circuit Sensor Model:

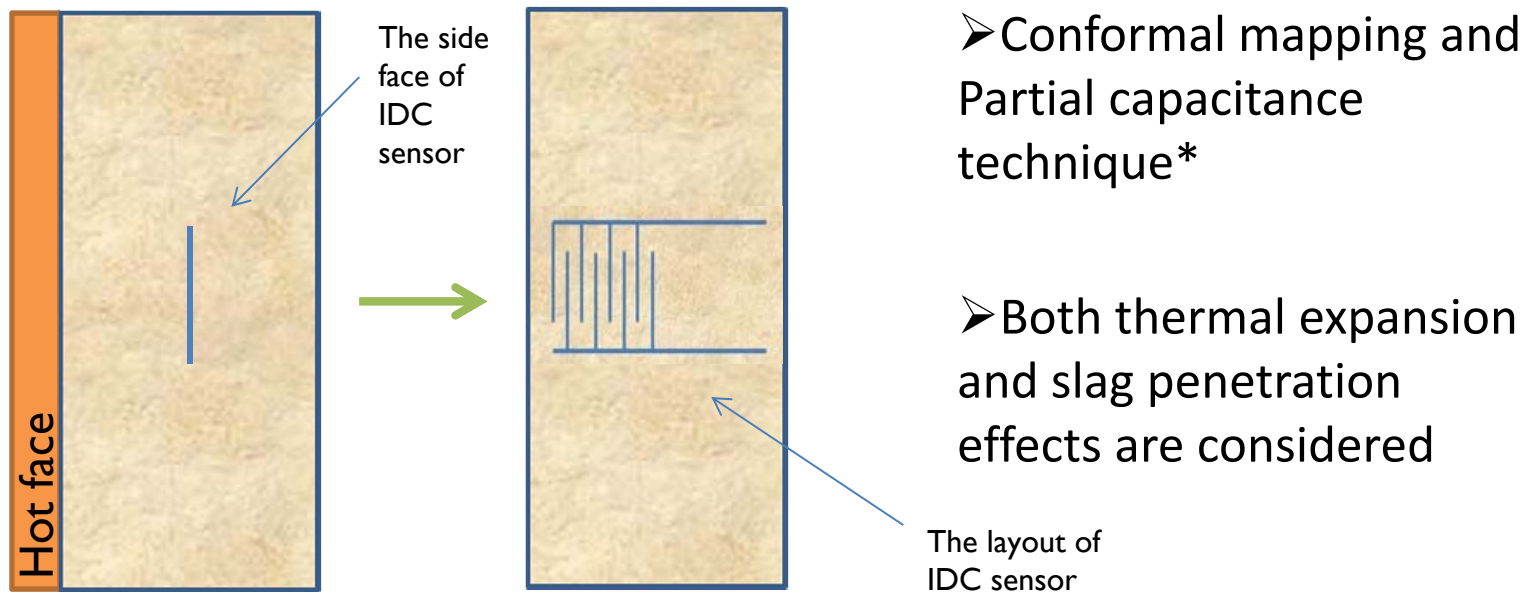


- The output resistance of the sensor depends on the temperature
- Equivalent circuit approach is used
- The electrical conductivity of slag is much smaller than the sensor ( $0.192\Omega^{-1}cm^{-1}$  vs  $44.57\Omega^{-1}cm^{-1}$ )
- Sensitivity analysis to temperature shows potential for temperature estimation



# Interdigital Capacitor (IDC) Sensor Model:

- The output capacitance can change with the temperature
  - Dielectric constant change due to physico-chemical changes in the refractory material and due to slag penetration
  - Thermal expansion (the geometry of sensor changes)
- Slag penetration can impact both the dielectric constant and the layout of the IDC.



\* Igreja R, Dias C.J. Analytical evaluation of the interdigital electrodes capacitance for a multi-layered structure, Sensors and Actuators A: Physical, 2004, 112(2): 291-301.

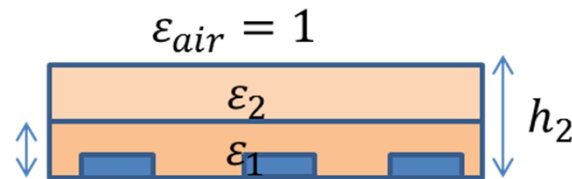


# IDC Sensor Model:

## Partial capacitance\*

- Different dielectric constant in the plane above and below the electrode level
- Each layer above or under the sensor plane (within a certain distance) will have a contribution to the total capacitance.

Example:



According to the partial capacitance technique, the total capacitance of this two-layered IDC is :

$$C_u = C_{h=\infty} + (\epsilon_1 - 1)C_{h=h_1} + (\epsilon_2 - \epsilon_1)C_{h=h_2}$$

\* Igreja R, Dias C J. Analytical evaluation of the interdigital electrodes capacitance for a multi-layered structure, Sensors and Actuators A: Physical, 2004, 112(2): 291-301.



# IDC Sensor Model:

- Mixing rules investigated in the study<sup>1,2,3</sup>:

$$\text{Rule\#1: } \varepsilon_r = \sum V_i \varepsilon_i^\alpha + V_p$$

$$\text{Rule\#2: } \varepsilon_r^{\alpha_1(1-f)+\alpha_2f} = (1-f)\sigma_M^{\alpha_1(1-f)+\alpha_2f} + f\sigma_A^{\alpha_1(1-f)+\alpha_2f}$$

$$\text{Rule\#3: } \frac{\varepsilon_r - 1}{3\varepsilon_r} = \sum \frac{V_i(\varepsilon_i - 1)}{\varepsilon_i + 2\varepsilon_r}$$

[1] Sun Y, Han J, Zhang Y. Relative dielectric constant calculation model for three-phase porous composite materials. *Computational Materials Science*, 2009, 45(4): 1125-1128.

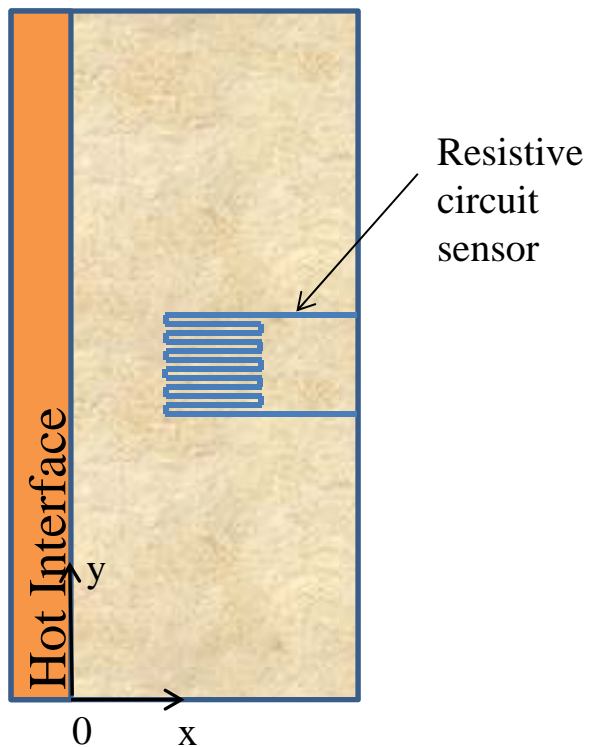
[2] Uvarov N F. Estimation of composites conductivity using a general mixing rule. *Solid State Ionics*, 2000, 136: 1267-1272.

[3] Fang Y C, Jean J H. Compositional design of lead-free, low-temperature co-fired ceramic dielectric composite. *Japanese Journal of Applied Physics*, 2006, 45(8R): 6357.



## Strain Sensor Model:

- Combined effect of thermal stress and stress developed due to physical and chemical changes can be captured by the strain sensors.

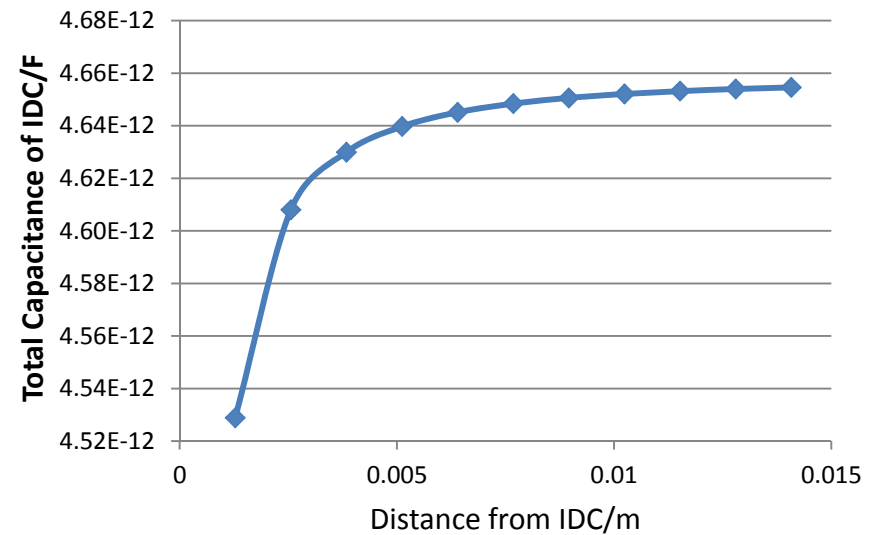
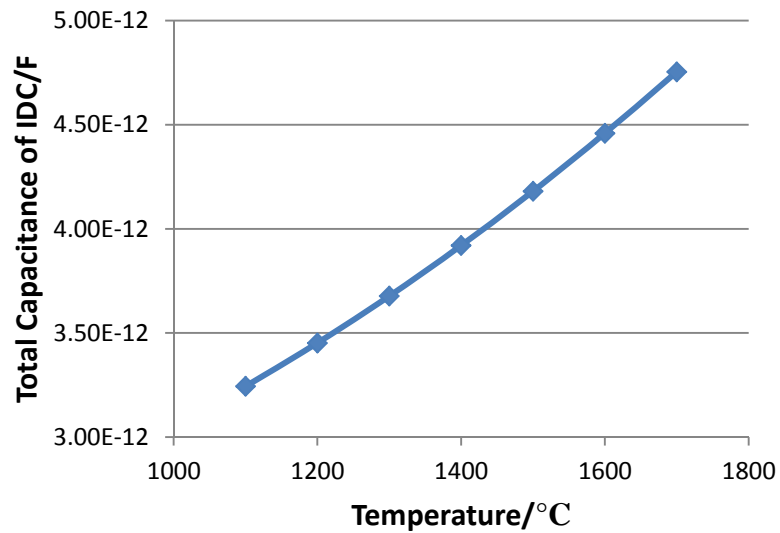


- The output electrical resistance of the sensor depends on:
  - Deformation of the sensor
  - Change in the electrical conductivity
- Temperature-dependent data for Young's modulus and Poisson's ratio obtained from open literature for alumina



# Results:

## Interdigital Capacitor (IDC) Sensors

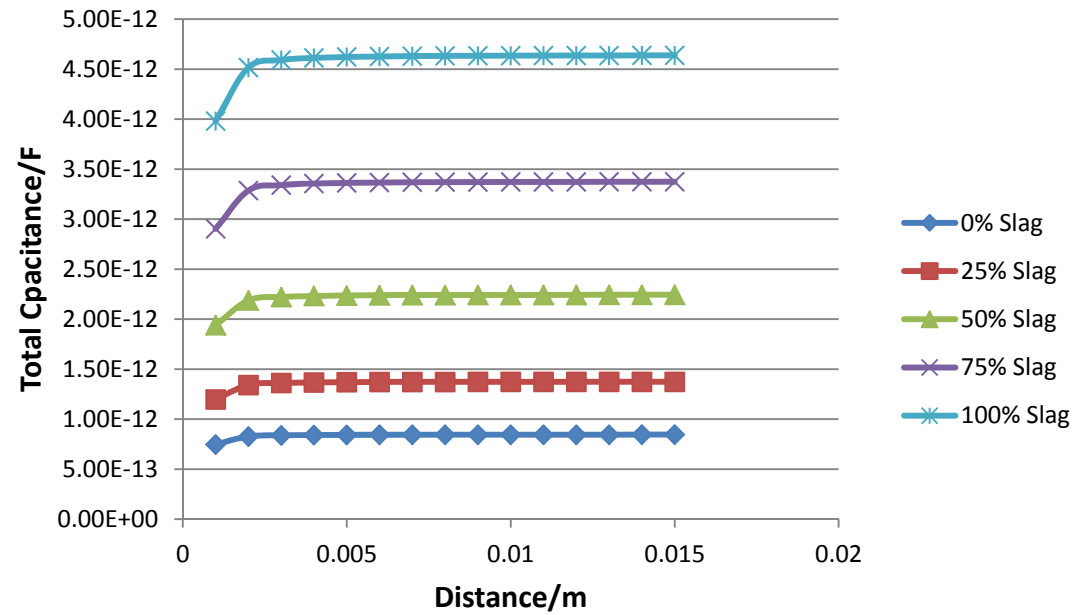




# Results

## Interdigital Capacitor (IDC) Sensor Model

Rule#1:



# *Development of Filtering Algorithm:*

- Estimation problem (DAE system):

$$\dot{x} = \bar{F}(x, z) + \gamma$$

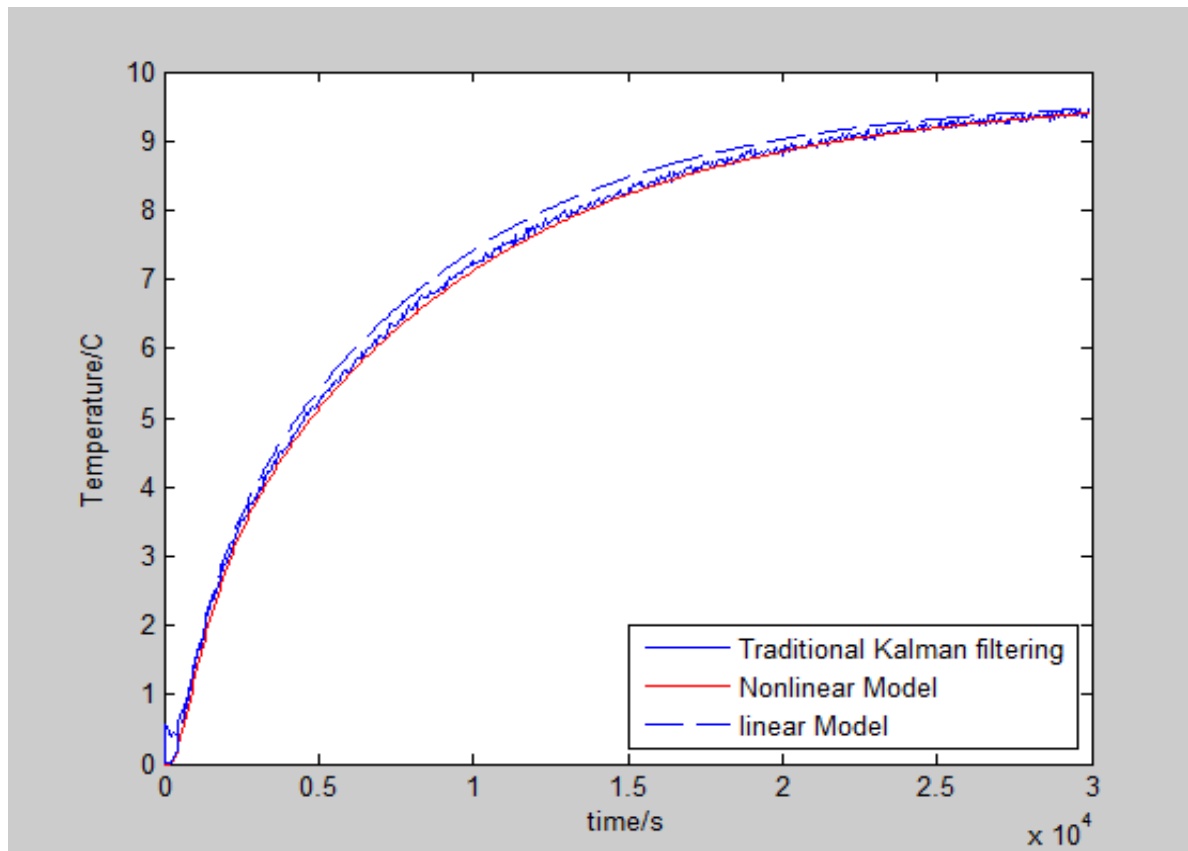
$$\bar{0} = \bar{G}(x, z)$$

$$Y = H \begin{bmatrix} x \\ z \end{bmatrix} + \omega$$

- Developed approach for handling the DAE System
- Initial testing with the traditional Kalman filter
- All models and algorithms implemented in MATLAB



## *Results from Traditional Kalman Filter:*



- Use the measurements from the thermocouple to estimate the temperature
- Sensor placed considering physical limitations
- Sensor placement locations are flexible



## *Task 6 Conclusions and Future Work:*

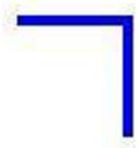
- All the models for the smart refractory with embedded sensors have been developed (**M9**). It appears that while all sensors show sensitivity to the temperature, only the model of the embedded IDC show considerable sensitivity to slag penetration.
- Development of traditional Kalman filter completed
- Future work will focus on validation of the sensor models with the experimental data
- Work will continue on development of the nonlinear unknown input filter for measurements from a wireless network
- Developed filtering algorithms will be tested using experimental data



# Acknowledgements:

- We would like to thank **U.S. Department of Energy (DOE)** for sanctioning this project **DE-FE0012383**.
- Dr. Maria Reidpath, U. S. Department of Energy, is greatly appreciated for her insight and valuable guidance.
- We also would like to acknowledge Dr. Wei Ding and Dr. Marcela Redigolo and Dr. Kollin Brown and Mr. Harley Hart for their cooperation and valuable assistance in the WVU Shared Facilities.
- Thanks are also due for Mr. Timothy Close, Harbinson Walker International for the technical support.
- Kindly acknowledge Faculty and staff of Department of Mechanical and Aerospace Engineering, West Virginia University for their support.



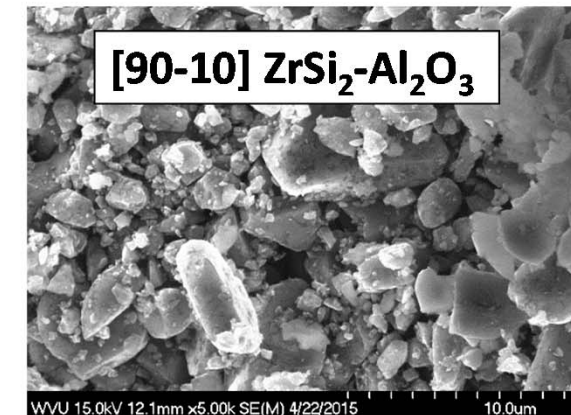
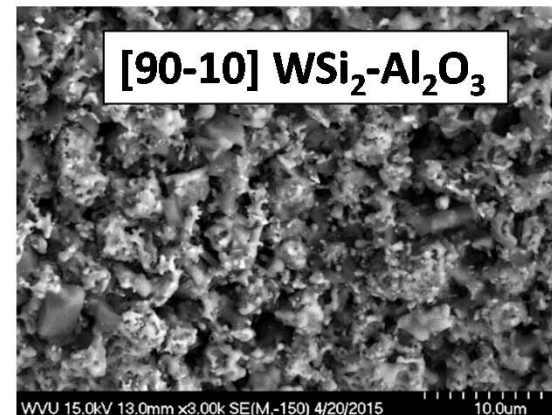
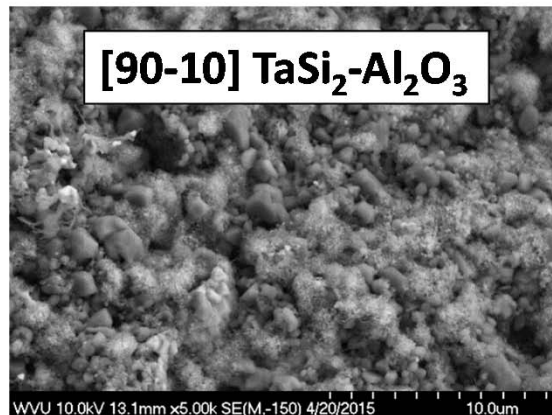
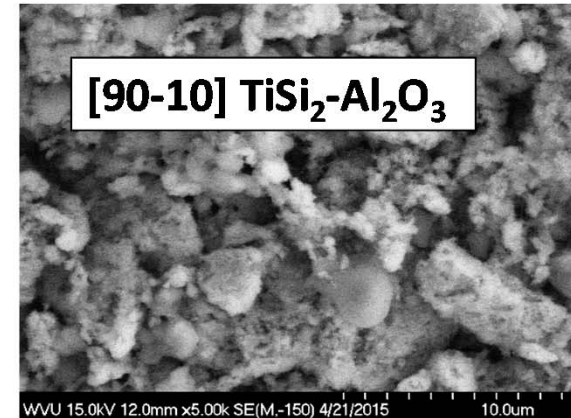
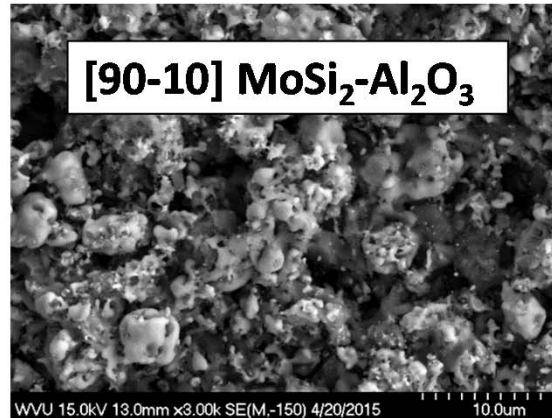
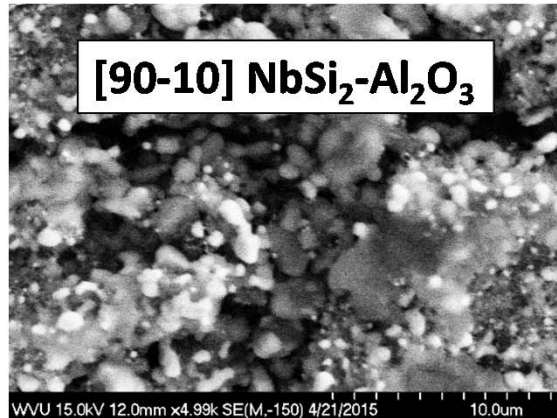


*Appendix:*



# Thermocouple Microstructures:

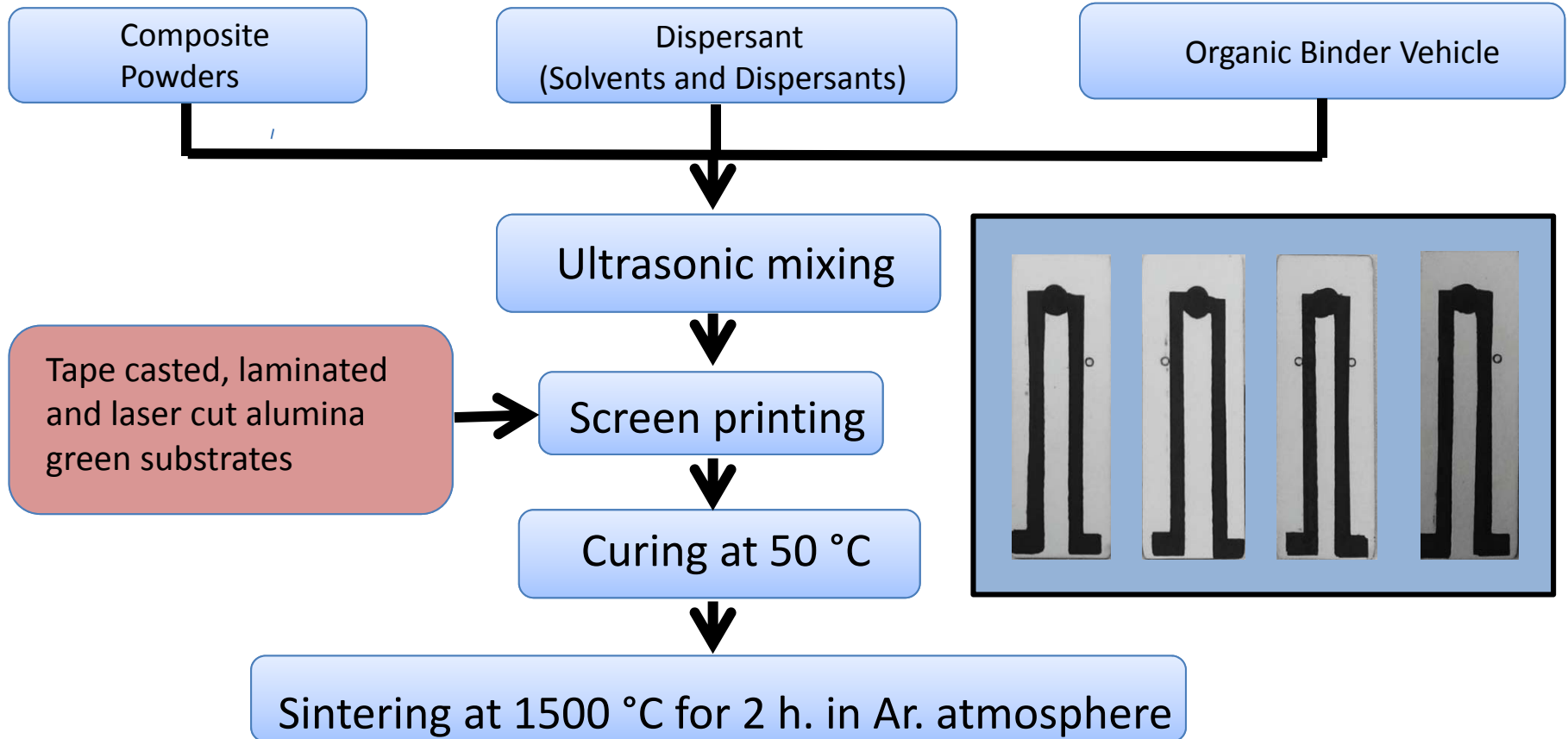
Microstructure of ceramic-ceramic thermocouples sintered at 1500 °C in argon



The SEM micrographs clearly shows that the thermocouples are fully dense and hence improves the conductivity

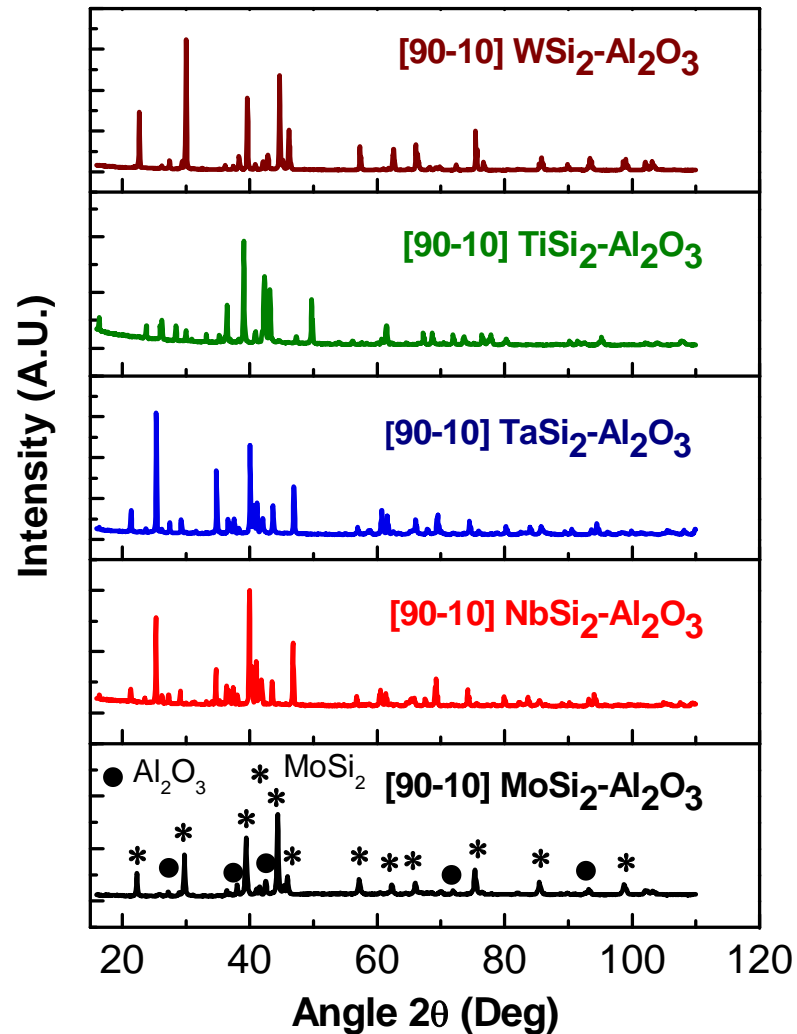


# Embedded Thermocouple Preform:





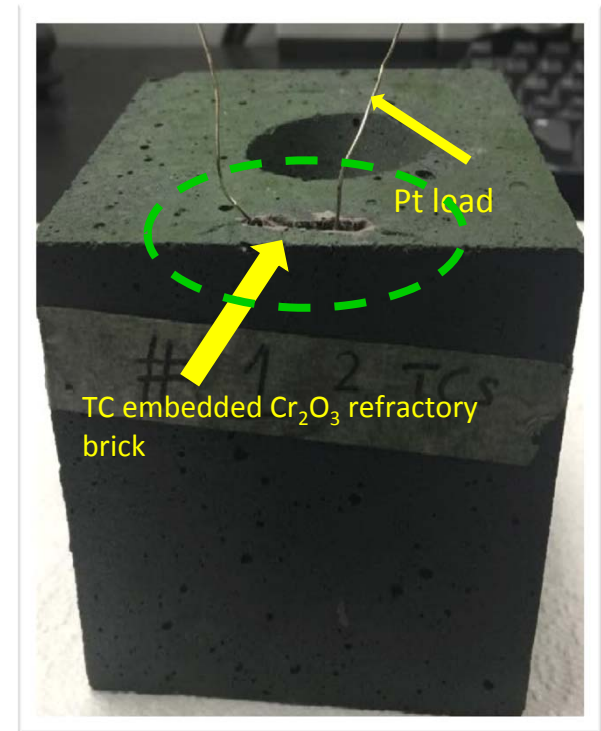
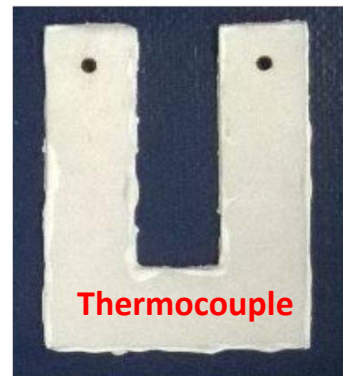
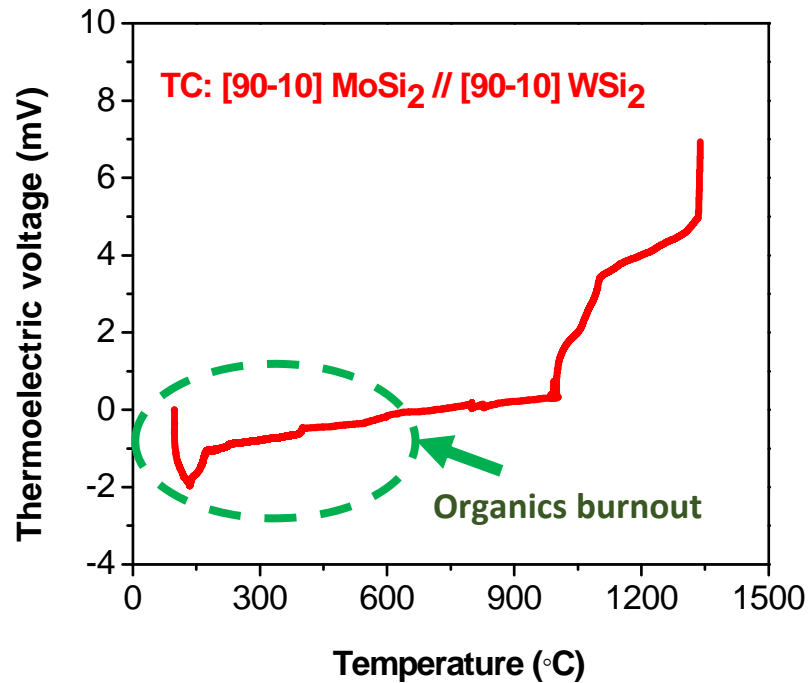
# Thermocouple Microstructures:



X-ray analysis of various ceramic-ceramic thermocouples sintered at 1500 °C in Ar

# Smart Refractory Performance:

Investigation of corrosion/erosion kinetics in static mode



The thermocouple with composition [90-10] vol% MoSi<sub>2</sub>-Al<sub>2</sub>O<sub>3</sub> // [90-10] vol% WSi<sub>2</sub>-Al<sub>2</sub>O<sub>3</sub> embedded within the Cr<sub>2</sub>O<sub>3</sub> refractory was tested from room temperature to 1400 °C in argon atmosphere.



# Ceramic Testing Stress/Strain Sensors:

- Introduce 10% oxygen flow into furnace during burnout of imbedded sensors to eliminate carbon deposits
- Texture substrates in the gripper area to prevent slipping during testing
- Amend sensor design to increase Gauge Factor
- Evaluate temperature effects on strain sensor
- Initiate compressive testing of ceramic strain sensors

Design ID	A	B	C
	(mm)	(mm)	(mm)
V3	40	1.0	1.0
V4	40	0.5	1.0
V5	40	0.5	0.5
V6	40	0.2	1.0
V7	40	0.2	0.5

**A – Sensor length**

**B – Spacing between legs**

**C – Leg width**

